Title
Mechanical and physiological determinants of elastic energy storage

Author
Mendoza, Elizabeth

Publication Date
2023

Peer reviewed|Thesis/dissertation

UNIVERSITY OF CALIFORNIA,
IRVINE

Mechanical and physiological determinants of elastic energy storage

DISSERTATION

submitted in partial satisfaction of the requirements
for the degree of

DOCTOR OF PHILOSOPHY

in Biological Sciences

by

Elizabeth Mendoza

Dissertation Committee:
Associate Professor Emanuel Azizi, Chair
Associate Professor Matthew McHenry
Assistant Professor Natalie Holt

2023

DEDICATION

To

my family

for their endless love and support.

TABLE OF CONTENTS

LIST OF FIGURES

LIST OF TABLES

ACKNOWLEDGEMENTS

I would like to thank my advisor, Dr. Manny Azizi, for his mentorship and guidance. Thank you for encouraging me and always being so excited about my work. Thank you to my committee members, Drs. Natalie Holt and Matt McHenry, for their invaluable feedback and guidance. Thank you to Drs. Monica Daley and Kelli Sharp for serving on my advancement committee and supporting me through that difficult experience. Thank you to the UCI Physiology Group for creating a space to grow and develop as a scientist and for providing invaluable feedback and professional development experiences. Thank you to the Impulsive MURI team and specifically to Dr. Sheila Patek for creating such an engaging space to be a young scientist. Working with the Impulsive MURI team was one of the highlights of my PhD experience. Thank you to Drs. Christopher Richards and Janneke Schwaner for help with methods from Chapter 3.

I would like to thank my lab mates for being so supportive and creating a welcoming lab environment. Thank you to Dr. Jeff Olberding for taking me under his wing and teaching me all things frog muscle preps. Thank you to Adrien Arias and Dr. Alex Duman for being supportive lab mates and for always being willing to help. Thank you for your friendship and the fun adventures we had together. I love you guys. Thank you to the amazing undergraduate researchers I was privileged to mentor. Dustin, Rebecca, Emily, Malia, and Maya – thank you for choosing me as your research mentor and for injecting new energy and excitement.

Thank you to all the people I am lucky enough to call friends. Thank you to Sarah, Audrey, Adrien, Alex, Dean, Jo, Daisey, Po, Karen, and Vivi for being there through my worst and best times. Thank you for being a shoulder to cry on and for listening to me vent for days about things that were bothering me. Thank you for celebrating me on my accomplishments and for always making me feel loved.

Thank you to my best friend in the whole wide world, Miss Luna. Luna is my dog and she'll never be able to read this, but she was there since day one. Luna forced me to slow down and smell the roses, and to detach from work stress. Thank you Lunitunes for all the wet kisses and cuddles.

Lastly, I'd like to thank my family. Gracias a mis padres por todos sus sacrificios y por darnos todo lo que pudieron darnos. Gracias por siempre apoyarme en mis metas. Todos mis logros son para ustedes. Thanks to my siblings for always making me laugh and for supporting me in all my endeavors. I love you.

Chapter 1 is a reprint of the material as it appears in Mendoza, E., and Azizi, E. (2021). Tuned muscle and spring properties increase elastic energy storage. *Journal of Experimental Biology, 224*(24), jeb243180, used with permission from The Company of Biologists. The co-author listed in this publication is Emanuel Azizi. This dissertation was supported by the U.S. Army Research Laboratory and the U.S. Army Research Office under contract/grant number W911NF-1510358.

VITA

Elizabeth Mendoza

2011 – 2015 B.S. Biology, University of California, Riverside

2016 – 2018 M.S. Zoology, Oklahoma State University

2018 – 2023 Ph.D. Biological Sciences, University of California, Irvine

Field of Study

Skeletal muscle physiology, comparative biomechanics, and animal locomotion

PUBLICATIONS

5. **E. Mendoza**, D. S. Moen, and N. C. Holt. The importance of comparative physiology: mechanisms, diversity, and adaptation in skeletal muscle physiology and mechanics. *Journal of Experimental Biology*. 226, jeb245158.

4. N. P. Hyun, J. P. Olberding, A. De, S. Divi, X. Liang, E. Thomas, R. St. Pierre, E. Steinhardt, J. Jorge, S. J. Longo, S. Cox, **E. Mendoza**, G. P. Sutton, E. Azizi, A. J. Crosby, S. Bergbreiter, R. J. Wood, S. N. Patek. Spring and latch dynamics can act as control pathways in ultrafast systems. *Biomimetics and Bioinspiration*. In press.

3. **Mendoza E** and Azizi E. (2021). Tuned muscle and spring properties increase elastic energy storage. *Journal of Experimental Biology*, 224, jeb243180.

2. **Mendoza, E**, Azizi E, and Moen DS. (2020). What explains vast differences in jumping power within a clade? Diversity, ecology and evolution of anuran jumping power. *Functional Ecology*, 34, 1053–1063.

1. Sutton GP, **Mendoza E**, Azizi E, Longo SJ, Olberding JP, Ilton M, and Patek SN. (2019). Why do large animals never actuate their jumps with latch-mediated springs? Because they can jump higher without them. *Integrative and Comparative Biology*, 59, 1609–1618.

In Revision

1. **Mendoza, E.**, Martinez, Maya, Olberding, J. P., and Azizi, E. Temperature effects on elastic energy storage and release in a system with a dynamic mechanical advantage latch. *In review with the Journal of Experimental Biology. 05/09/2023.*

ABSTRACT OF THE DISSERTATION

Mechanical and physiological determinants of elastic energy storage

by

Elizabeth Mendoza

Doctor of Philosophy in Biological Sciences

University of California, Irvine, 2023

Associate Professor Emanuel Azizi, Chair

The fastest biological movement are capable of generating high mechanical power efficiently and repeatably. Many of the fastest movements are achieved by using a common mechanistic framework know as latch-mediated spring actuation (LaMSA). While the fundamental mechanisms associated with LaMSA have been described over the last decade, such advances have not yet been able to pinpoint the mechanical or physiological features that explain biological variation in whole system performance. Furthermore, predicted scaling relationships suggest that there is a continuum between elastic recoil use and direct muscle actuation where elastic recoil is most prevalent at small masses and organisms transition to direct muscle actuation at large sizes. These predictions provide a framework that motivates experimental approaches aimed at understanding how animals at intermediate size range partition direct muscle and spring actuation to power fast movements.

In this dissertation, I investigated factors that influenced energy storage and energy release in frogs who are believed to use both LaMSA and direct muscle actuation to power jumping. First, I examined interspecific variation in the *plantaris longus* muscle-tendon unit (MTU) of three species of frogs to investigate how tuned properties of the MTU affected their capacity to store energy. I found that high energy storage capacity was achieved when both muscle force capacity and relative spring stiffness increased. Second, I investigated how a dynamic mechanical advantage latch affected energy storage and energy release while varying environmental temperature. I found that the while spring actuation accounts for a significant portion of the energy of a jump, muscles continue to contribute energy during spring actuation. The ability to contribute this mechanical energy during the actuation phase required high muscle power and therefore explained the thermal sensitivity observed in these systems. Lastly, I examined the energy stored and returned during frog jumps. I discovered that the muscle stored energy in elastic structures prior to any substantial movement, and that it contributed work to the jump during limb extension. I found that 70% of the total muscle fascicle work was done during the loading phase and 30% was done during the unloading phase. Taken together, my dissertation work demonstrated that variation in elastic energy storage and release could be a consequence of evolutionary differences, latch mechanics, and real time control of energy flow.

INTRODUCTION

Movement is critical to the survival and reproduction of most animals (Biewener and Patek 2018). Animals move short and long distances to find resources (e.g. food, water, and shelter), to find mates, and compete for mating opportunities. Moving fast can be especially important for capturing prey or evading predators. The speed at which animals move is determined by the contractile capabilities of underlying skeletal muscle driving the movement. These contractile capabilities are dependent on the overlap and rate of cycling of the contractile unit of skeletal muscle, molecular filaments actin and myosin. To produce force actin and myosin must overlap to allow for crossbridge formations. The amount of overlap between the filaments dictates how much force can be produced. If there is no overlap, then no crossbridges can form and no force is produced. If they overlap too much, the filaments interfere with one another and crossbridge formation cannot occur, and no force can be produced. However, if there is intermediate overlap, then an optimal amount of crossbridges could form and substantial force could be generated. This relationship characterizes the force-length property of skeletal muscle (Gordon et al. 1966). Moreover, the contractile capabilities of skeletal muscle are also dependent on the rate of crossbridge cycling. If crossbridge cycling is fast, low forces will be produced. If crossbridge cycling is slow, high forces will be produced. This relationship characterizes the force-velocity relationship of skeletal muscle (Hill 1938). Together, the force-length and force-velocity relationships determine the contractile capabilities of skeletal muscle and ultimately the speed at which animals move.

Yet, some organisms perform exceptionally fast movements that exceed the contractile capabilities of skeletal muscle and deliver large amounts of energy over a short period of time (i.e., they are high powered) by using latch-mediation spring-actuation mechanisms (or elastic

recoil mechanisms) (Ilton et al. 2018; Longo et al. 2019; Patek 2023). For this mechanism to work a *latch* must resist motion to allows work done by the muscle (or *motor*) to be temporarily stored as potential energy in the deformations of *elastic structures* (e.g., tendon, aponeurosis, apodeme, springs; Alexander 1988; Biewener and Patek 2018). Then, through mediation by the *latch* this stored energy is quickly released via recoil of elastic structures launching the *projectile* (Ilton et al. 2018; Longo et al. 2019; Patek 2023). A hallmark of this mechanism is the temporal and spatial decoupling of muscle contraction from motion which is thought to permit the muscle to contract in or near ideal conditions for force generation. Moreover, because elastic structures are not limited by enzymatic processes, they are able to deliver stored energy at rates faster than the rates at which they were generated (Patek 2023).

Historically, organisms that used elastic recoil mechanisms were identified by calculating a ratio of movement power to muscle power. When movement power exceeded muscle power the behavior was deemed 'power amplified' or driven by recoil of elastic structures. Through this approach many organisms were identified as users of elastic recoil mechanisms demonstrating that it was widespread and varied within and across species (Aerts 1998; Patek et al. 2004; Anderson and Deban 2010; Roberts and Azizi 2011; Patek et al. 2011; Deban and Richardson 2011; Henry et al. 2015; Ilton et al. 2018; Longo et al. 2019; Sutton et al. 2019; Deban et al. 2020; Mendoza et al. 2020; Deban and Anderson 2021; Patek 2023). Moreover, modeling and empirical studies showed that elastic recoil scaled with mass where the smallest organisms were found to use elastic recoil mechanisms, the largest organisms were found to use direct muscle for movements, and the intermediate mass organisms were found to use both (Ilton et al. 2018; Sutton et al. 2019; Mendoza et al. 2020). Thus, scaling is a critical piece in LaMSA mechanisms, yet the general understanding of why or how variability arises remains unknown. In 2019, Longo

and colleagues proposed that to understand why and how variability in elastic recoil mechanisms arose we needed to shift our focus away from the power output of movements and muscles, and instead towards examining the interactions and mechanics of the elastic recoil components (i.e., motor, spring, latch, projectile). Through this proposed framework, termed latch-mediation spring-actuation (LaMSA), the authors suggested that we could interrogate the flow of energy by parsing out the movement into distinct phases (i.e., latching, spring loading, latched, spring actuation, and ballistic) to more rigorously understand how interactions between the components resulted in exceptional performance. Moreover, the authors demonstrated that by using this framework we could unify biological (e.g., animals and plants) and synthetic systems and examine them through the lens of LaMSA to look for governing principles.

LaMSA mechanisms are believed to be responsible for thermally robust movements observed in some ectothermic organisms. This is illustrated when examining the temperature coefficient, Q_{10}, a metric that shows the rate of change of a variable when temperature is increased by 10°C. A Q_{10} of 1.0 indicates that the variable of interest is independent of temperature change, a Q_{10} of 2.0 indicates that the variable increases by two-fold over the temperature range, and a Q_{10} of 0.5 indicates that the variable is halved over the temperature range. Contractile rates in skeletal muscle (e.g. rate of force development, contractile velocity, and power) typically display Q_{10} values of 1.5 – 3.0 (Bennett 1984; Rome 1990), whereas chameleon tongue projection performance (e.g. peak tongue velocity, acceleration, and power) showed Q_{10} values of 1.1 - 1.3 demonstrating that tongue projection performance was less sensitive to changes in temperature than what would be expected based on the temperature effects of muscle alone (Anderson and Deban 2010). This phenomenon has been observed in salamander, frog, and toad tongue projection and ballistic mouth opening (Deban and Lappin

2011; Deban and Richardson 2011; Sandusky and Deban 2012; Scales et al. 2017; Deban et al. 2021). Yet, other movements like jumping in crickets (Deban and Anderson 2021) and frogs (Hirano and Rome 1984) were shown to be sensitive to changes in temperature despite use of elastic recoil mechanisms. Thus, our understanding of the aspects that lead to thermal robustness through use of LaMSA mechanisms remains poorly understood.

In this dissertation, I investigated mechanical and physiological factors that affected elastic energy storage and return in the *plantaris longus* muscle-tendon unit of anurans (frogs and toads). I focused on this muscle because it is known to be involved in elastic recoil during frog jumping, and elastic recoil use has been shown to vary across species (Azizi and Roberts 2010; Astley and Roberts 2012, 2014; Astley 2016; Mendoza et al. 2020). Additionally, frogs are thought to be in the transition zone between elastic recoil use and direct muscle movements suggesting that the mechanics of the energy release may be more complex (Ilton et al. 2018; Sutton et al. 2019).

SUMMARY OF WORK

Using this framework, this work aimed to understand how components of the elastic recoil mechanism contributed to variability in elastic energy storage and return. We focused these studies on the *plantaris longus* muscle-tendon unit of frogs.

In chapter 1, we used the *plantaris longus* muscle-tendon unit of Cuban tree frogs (*Osteopilus septentrionalis*), Cane toads (*Bufo marina*), and American bullfrogs (*Rana catesbeiana*) to determine how natural variability in morphology and physiological properties of the muscle-tendon unit resulted in energy storage. We instrumented the muscles with sonomicrometry and used muscle ergometry to characterize the force-length property of these muscles. Using this approach, we related physiological properties of the muscle-tendon unit with

the natural variability arising across species. We showed that the Cuban tree frog could store more energy than the other two species, which was consistent with jump performance observations. We found that they could do this because they had muscles that could generate more force per unit muscle mass because they packed more contractile units into the muscle volume through higher pennation angles, and they had stiffer elastic structures that allowed for more energy to be stored. Our results suggest that tuning the components of the LaMSA mechanism maximized the capacity for elastic energy storage.

In chapter 2, we used a novel experimental approach to test how a dynamic mechanical advantage latch influenced elastic energy storage and return while varying environmental temperature. We used an isolated muscle preparation of the *plantaris longus* muscle-tendon unit of American bullfrogs. We coupled this preparation with a computer model of a simplified jumper using a real-time feedback controller and we ran these preparations at 10, 15, 20, and 25°C. We found that the energy stored and returned by elastic recoil was temperature sensitive. We found that the muscle continued to contribute work after unlatching, and this contribution was extremely sensitive to changes in temperature. Our results indicated that temperature sensitivity observed in the energy stored and returned by elastic recoil was a consequence of the unlatching mechanics. Moreover, additional contributions by the muscle after unlatching exasperated the temperature effects.

In chapter 3, we used in vivo muscle techniques to measure elastic energy storage and return in American bullfrog jumps. We instrumented bullfrogs with sonomicrometry and leaf-spring tendon buckles to measure muscle fascicle length and muscle force, respectively. Instrumented frogs were jumped from a platform, and we recorded in vivo muscle measurements with three-dimensional high-speed video, simultaneously. We found that the frog jumping

mechanism generally followed the idealized LaMSA framework with some key deviations that were a consequence of the latch. We found that the *plantaris longus* muscle stored energy in elastic structures prior to any appreciable ankle movement, and continued to contribute work during ankle joint extension demonstrating that frog jumps were driven by both LaMSA mechanisms and direct muscle actuation. Our work showed that on average 70% of total muscle work was done by the *plantaris longus* muscle during the loading phase and 30% was done during the unloading phase. This work was the first to characterize the flow of energy in a LaMSA system and demonstrated how the latch mediated energy flow and could introduce variability in elastic energy storage and return.

CHAPTER 1

Tuned muscle and spring properties increase elastic energy storage

INTRODUCTION

Fast and powerful movements like the jump of a flea (Bennet-Clark and Lucey 1967) or the strike of a mantis shrimp smasher (Patek and Caldwell 2005) are possible because they use elastic energy storage mechanisms, or latch-mediated spring-actuation (LaMSA; Longo et al. 2019). In this mechanism a latch resists motion of a limb segment (or appendage) while allowing loading muscles to contract slowly and forcefully to store mechanical energy (i.e., work) in the deformations of elastic structures (e.g. tendon, aponeurosis, or apodeme; Alexander 1988). Upon the removal or release of the latch, the elastic structures recoil delivering stored energy at rates faster than what muscle could do alone (Ilton et al. 2018; Longo et al. 2019; Abbott et al. 2019).

In LaMSA, the temporal decoupling of muscle contraction from movement reduces the shortening velocity of contracting muscles enabling them to contract against elastic structures with high force. While this decoupling allows loading muscles to operate at a higher proportion of their force capacity, recent evidence also suggests selection has acted to enhance maximum force capacity of muscles used in LaMSA. For example, the loading muscles of LaMSA systems in some organisms have long resting sarcomere lengths and large physiological cross-sectional areas indicating potential selection for high muscle force capacity (Mendoza-Blanco and Patek 2014; Larabee et al. 2017; Booher et al. 2021). Yet it remains unknown whether increased force capacity occurs in the loading muscles of vertebrate systems that use elastic recoil to power

movement. The relatively little variation in resting sarcomere length (~2μm; Burkholder and Lieber 2001) in vertebrate muscle suggests that to increase the force capacity of muscle they may be constrained to changes in PCSA - either through changes in mass, pennation angle, or both. An increase in mass should result in an increase in force. In particular, an increase in mass would result in a proportional change in PCSA, and because the force generating capacity of muscle is a function of PCSA, force would also increase. Furthermore, if the pennation angle of a muscle were relatively higher, more fascicles with shorter lengths could be packed into the volume of the muscle, resulting in an increase in PCSA and a net increase in force generating capacity (Sacks and Roy 1982; Otten 1988; Azizi et al. 2008; Biewener and Patek 2018).

Effective tuning of muscle and spring force capacities is essential for effective function of LaMSA systems (Ilton et al. 2018). Any change in muscle force should be accompanied by a tuned change in spring stiffness to increase elastic energy storage capacity. A spring stiffness matched to the force capacity of the energy loading muscle would allow it to operate along lengths (in the force-length curve) ideal for generating high force and elastic energy storage. Thus, if a muscle contracts against a spring that is not matched to its force capacity, then less energy will be stored. For example, if a muscle contracts against a spring that is relatively too compliant while the latch is engaged, then the muscle would shorten to a sub-optimal length which would result in more muscle excursion and a reduction in force generation (Fig. 1.1a). If instead a muscle contracts against a spring that is relatively stiff while the latch is engaged, then the muscle will shorten very little and store less energy because it cannot deform the elastic structures (Fig. 1.1a). Thus, based on theoretical considerations, any change in a muscle's force capacity would need to be accompanied by a corresponding shift in the mechanical properties of elastic structures.

Frogs are an ideal comparative animal model for investigating functional shifts in muscle-spring tuning in elastic recoil systems. Jumping power varies substantially across frog species and its been shown that smaller species tend to jump with higher muscle-mass-specific power (Roberts et al. 2011; Astley 2016; Mendoza et al. 2020). Frogs also happen to occupy a size range that is considered transitional such that the performance benefits of spring actuation (relative to direct muscle actuation) may be limited, potentially explaining the performance variation observed in the clade (Sutton et al. 2019). In addition, the LaMSA mechanism used by frogs (Roberts and Marsh 2003) provides the possibility of simultaneously using a combination of both spring and muscle actuation to power jumps by allowing muscles to contribute additional work during limb extension (Sutton et al. 2019; Olberding et al. 2019). The mechanistic diversity observed in frogs provides a unique opportunity to link the properties of LaMSA components to overall jump performance.

In frogs, the *plantaris longus* muscle-tendon unit (MTU) is an important site of elastic energy storage (Astley and Roberts, 2012; Astley and Roberts 2014). Here we used isolated muscle preparations of the *plantaris longus* MTU to assess the tuning of muscle force capacity and spring properties. We examined the *plantaris longus* MTU of three species of frogs that vary in jumping power, but not isolated muscle power (Roberts et al. 2011). Moreover, we used this preparation to test whether species differed in energy storage capacity at the *plantaris longus* MTU. We hypothesized that MTUs that have the highest energy storage capacity will show increased force capacity to the muscle, and spring properties tuned to high muscle force capacity.

METHODS

Animals

Six bullfrogs (*Rana catesbeiana*), five cane toads (*Rhinella marina*), and four Cuban tree frogs (*Osteopilus septentrionalis*) were purchased from herpetological vendors (Table 1.1). All animals were adults. They were housed individually in large aquaria and were fed calcium-supplemented crickets *ad libitum*. Animal husbandry and use were approved by the University of California, Irvine Animal Care and Use Committee (Protocol AUP 20-129).

In-vitro preparation

Animals were euthanized with a double-pithing protocol prior to the isolation of the muscle tendon unit (MTU). In this study we followed experimental procedures outlined in Azizi and Roberts (2014). First, we removed the skin from the upper hind limb exposing the musculature. Then, we carefully isolated the sciatic nerve from surrounding tissue. Next, we removed the skin from the lower hind limb to expose the *plantaris longus* muscle. With a sapphire blade we carefully made a small incision between two fascicles in the most proximal region of the muscle. We used this incision to implant a sonomicrometry crystal (Sonometrics Corporation, London, ON, Canada). We made a second incision distal to the first sonomicrometry crystal (and proximal to the aponeurosis sheet) along the same two fascicles and implanted a second sonomicrometry crystal. We secured the crystals with 6-0 silk. After instrumentation, we detached the distal tendon from the plantar fascia while keeping the muscle attached to the isolated knee joint. The isolated MTU preparation was secured to a rigid clamp at the knee joint and the distal tendon was placed in a custom-made clamp. The clamp on the distal tendon was attached to a servomotor (310C, Aurora Scientific, Cambridge, MA, USA). Once the MTU was tightly secured, it was placed in a bath of Ringer's solution that was continuously aerated with oxygen and kept at room temperature (22 ±1°C) . Finally, the sciatic nerve was

threaded through a custom-made nerve cuff that was connected to a Grass S88D stimulator (Grass Technologies, Warwick, RI, USA) and used to electrically stimulate the muscle.

Stimulation voltage was determined through twitch contractions. The stimulation voltage was increased by 1V increments until the twitch force plateaued (i.e., peak force stopped increasing). We set the stimulation voltage to 1V above that of which resulted in maximal twitch force to supramaximally stimulate the muscle (8-12V). Tetanic stimulations consisted of 0.2ms pulses at 80 pulses per second for durations of 400ms. We varied the length of each muscle before each tetanic contraction to characterize the force-length property. Because we varied the length of the muscle prior to stimulation we also characterized the passive force-length property. Changes in muscle fascicle lengths were measured with sonomicrometry, and the servomotor measured changes in force. Figure 1.
3 shows representative time series of these contractions for the *plantaris longus* muscle of all three species. All data were collected at 1000Hz using a 16-bit data acquisition system (National Instruments USB-6212). After the experiments, we measured muscle mass (in grams), fascicle length (in millimeters), and pennation angle (in degrees). We used these morphological parameters to calculate muscle PCSA assuming a constant muscle density of 1.056 g cm^{-3} (Mendez and Keys 1960).

Data Processing

Data were processed using Igor Pro software (Wavemetrics, Lake Oswego, OR, USA). The passive force-length curve of the muscle was constructed by plotting fascicle length against the passive force at each varied length prior to stimulation. Therefore, this relationship characterizes the passive properties of the muscle fascicles and not the MTU. Next, the passive

force-length data were fit with a standard exponential function following Azizi and Roberts (2010). The total force-length curve was constructed by plotting tetanic force against fascicle length. Note that because the fascicles of the *plantaris longus* insert into aponeurosis (a sheet-like tendon along the muscle belly), they shorten during tetanic contractions. Thus, fascicle length and force were measured where force plateaued (Fig. 1.2). The total force-length data were fit according to Otten (1987).

We calculated the work done by muscle fascicles during a series of tetanic contractions each starting at a different length. During our experiments the MTU maintained a constant length, so any shortening of the muscle fascicles resulted in an equal stretch of the elastic elements. Thus, to calculate work done we plotted fascicle length against tetanic force. The area under this curve corresponded to the work done during the contraction. Because we were interested in understanding the maximum work that could be generated by these muscles, we focused primarily on the contraction with the highest work output for each muscle. Note that we measured fascicle shortening at one fascicle, and thus made the assumption that all fascicles undergo similar displacements. Next, to measure the stiffness of the elastic elements we calculated the slope of fascicle length versus tetanic force curves and normalized them by muscle PCSA. We normalized by PCSA to account for size differences across the three species. Note that our method of normalization does limit comparisons with other studies. Furthermore, we measured elastic element stiffness from muscle fascicle shortening, and previous studies show evidence that this approach may be limiting due to the mechanical arrangement of muscle and elastic elements (see Herzog 2019; Zelik and Franz 2017; Arellano et al. 2019). For each muscle we measured stiffness of the elastic elements from the contraction with the highest work (Fig. 3). Finally, to compare the force generating capacity of these muscles across species we normalized

peak tetanic force by PCSA to calculate stress and by muscle mass to calculate mass-specific force.

Data analysis

All analyses were performed in R (http://www.R-project.org/). We ran an analysis of variance (ANOVA) on morphological and contractile variables to test for differences across species. Specifically, to test whether species differed in mass-specific stored energy we performed an ANOVA with mass-specific stored energy as the response variable and species as the effect. Additionally, to test whether species differed in elastic element stiffness we performed an ANOVA with normalized stiffness as the response variable and species as the effect. To test whether there were differences in muscle stress we performed an ANOVA with muscle stress as the response variable and species as the effect. Because normalizing force by PCSA accounts for variation related to mass or pennation angle, we performed two more ANOVAs to examine pennation angle and mass-specific peak force in isolation. We did this to understand whether there were differences in muscle architecture or force generating capabilities based on mass, and whether these differences could account for differences in energy storage capacity. One included mass-specific force as the response variable and species as the effect, and the other included pennation angle as the response variable and species as the effect. Lastly, we performed an ANOVA on normalized passive force (i.e., normalized as a percentage of P_o) across species. We used Tukey's honest significance test (HSD) post-hoc analyses to assess comparisons that were significantly different.

RESULTS

The average normalized passive muscle force of the *plantaris longus* at the contraction that produced the highest work was 10.20%, 7.54%, and 8.89% of P_o for Cuban tree frogs, cane toads, and bullfrogs, respectively. The *plantaris longus* muscle of bullfrogs reached an average peak total force of 21.44N, the *plantaris longus* muscle of cane toads reached an average peak total force of 15.84N, and the *plantaris longus* muscle of Cuban tree frogs reached an average peak total force of 9.57N.

We found that mass-specific stored energy was significantly different across species ($F(2,15) = 5.187$, $p = 0.019$; Fig. 1.4a). We found that the *plantaris longus* of Cuban tree frogs could store mass-specific energies averaging 53 $J/kg_{muscle\ mass}$, and the *plantaris longus* of cane toad and bullfrog stored an average of 22 $J/kg_{muscle\ mass}$ and 37 $J/kg_{muscle\ mass}$, respectively. Tukey HSD post-hoc analysis showed that mass-specific stored energy differed significantly between Cuban tree frogs and cane toads ($p = 0.015$), but not between Cuban tree frogs and bullfrogs ($p = 0.223$) or bullfrogs and cane toads ($p = 0.187$).

We additionally examined peak muscle stress because energy storage capacity depends on the ability to generate force. We found that peak muscle stress did not differ across species ($F(2,15) = 1.651$, $p = 0.225$; Fig. 1.4b), which was consistent with previous studies (Roberts et al. 2011). Moreover, because normalizing force by PCSA (i.e., to calculate muscle stress) accounts for variation in both pennation angle and muscle mass we also examined pennation angle and mass-specific peak force in isolation to understand whether there were differences in muscle architecture or force generating capabilities based on mass, and whether these differences could account for differences in energy storage capacity. We found that mass-specific peak force differed significantly across species ($F(2,15) = 32.61$, $p = 3.45e^{-06}$; Fig. 1.4c). Post-hoc analysis showed that mass-specific force was significantly different between Cuban tree frogs and

bullfrogs ($p = 4.30e^{-06}$), and between Cuban tree frogs and cane toads ($p = 1.50e^{-05}$), but was not significantly different between cane toads and bullfrogs ($p = 0.890$). Additionally, pennation angle differed significantly across species ($F(2,15) = 4.408$, $p = 0.031$; Fig. 1.4d). Tukey HSD post-hoc analysis showed that pennation angle was significantly different between Cuban tree frogs and cane toads ($p = 0.027$), but not significantly different between Cuban tree frogs and bullfrogs ($p = 0.095$) or bullfrogs and cane toads ($p = 0.622$). Normalized passive force was significantly different across species ($F(2,15) = 5.746$, $p = 0.014$). Post-hoc analysis showed that normalized passive force was significantly different between bullfrogs and Cuban tree frogs ($p = 0.013$), but it was not significantly different between cane toads and Cuban tree frogs ($p = 0.329$) or bullfrogs and cane toads ($p = 0.153$). Finally, normalized spring stiffness was significantly different across species ($F(2,15) = 6.049$, $p = 0.012$; Fig. 1.4e). Post-hoc analysis showed that normalized stiffness differed significantly between Cuban tree frogs and bullfrogs ($p = 0.012$), and between Cuban tree frogs and cane toads ($p = 0.027$), but not between bullfrogs and cane toads ($p = 0.961$).

DISCUSSION

The *plantaris longus* of Cuban tree frogs stored more elastic energy than that of the cane toads or bullfrogs (Figs 1.3-1.4). We found that the architecture of this muscle in the Cuban tree frogs enabled higher mass-specific peak forces. Furthermore, we found that the elastic structures in Cuban tree frogs were relatively stiffer than in other species, and well-matched to the force capacity of the muscle (Fig. 1.4). Thus, here we propose that the *plantaris longus* muscle in Cuban tree frogs was modified for high force generation, and that the surrounding elastic structures were tuned to the force of the muscle to increase energy storage capacity.

The observed increase in the mass-specific force capacity of the *plantaris longus* of Cuban tree frogs likely results from architectural changes (i.e., shorter more pennate fibers) that allow high force production over a small working range. We found that pennation angle was higher and muscle fascicle lengths were shorter in the *plantaris longus* of Cuban tree frogs than other species. This architectural arrangement allows more short muscle fascicles to be packed into the same muscle volume, which increases PCSA and mass-specific force (Sacks and Roy 1982; Otten 1988; Azizi et al. 2008; Biewener and Patek 2018). These changes in muscle architecture have implications for locomotor function. For instance, Rosin and Nyakatura (2017) showed that three hindlimb extensor muscles from a rodent jumper specialist had relatively shorter fascicle lengths and higher pennation angles than its non-specialist relative, which would allow for higher mass-specific forces important for jumping. Similarly, Dick and Clemente (2016) showed that varanid lizards mitigate musculoskeletal stresses associated with increased size through functional shifts in muscle architecture that promote higher force production (i.e., higher pennation angles and shorter fascicles). Moreover, in cursorial organisms the highly pennate architecture of the distal hind limb muscles functions to generate high force economically to facilitate elastic energy savings (Biewener 1998; Biewener and Roberts 2000). Therefore, vertebrate organisms can modify muscle function through changes to muscle architecture and PCSA that have implications for locomotion. Our work suggests that this pathway is also used to increase muscle force in vertebrate systems that use elastic recoil (or LaMSA) to increase elastic energy storage.

Tuning spring stiffness to muscle force capacity maximized energy storage. We found that the *plantaris longus* of Cuban tree frogs contracted against a spring that was relatively stiffer than that of the other species, and matched to the increased force capacity of its muscle. In frogs

the *plantaris longus* muscle operates on the descending limb of the force-length curve (Azizi and Roberts 2010) suggesting that shortening against a relatively stiffer spring would allow the muscle to shorten onto the plateau where the muscle could reach the highest peak forces. Furthermore, studies have shown that the *plantaris longus* muscle continues to shorten during limb extension (Azizi and Roberts 2010; Astley and Roberts 2012) suggesting that after energy storage the muscle would be at a length where it could contribute substantial work directly while contracting onto the ascending limb of the force-length curve (Olberding et al. 2019). Therefore, a spring tuned to the force capacity of the muscle would place the muscle in a position to generate high forces throughout the majority of the energy storage phase, and would result in more energy stored. In contrast, a spring not tuned to the force capacity of the muscle would result in less energy stored. For example, a spring that is relatively too compliant (i.e., not matched to the muscle's force capacity) would allow the muscle to shorten past the plateau and into a length where it would generate low force (Fig. 1.1). Alternatively, a spring that is relatively too stiff would result in very little muscle shortening and energy storage (Fig. 1.1). While our work suggests that a relatively stiffer spring maximizes energy storage, relatively compliant springs could be ideal in cases where the force capacity of the muscle is constrained (Rosario et al. 2016). Thus, to maximize energy storage spring stiffness should be tuned to the force capacity of the muscle.

In this study we examined the energy storage capacity of *plantaris longus* MTUs of three species of frogs that have been shown to differ in jumping power (Roberts et al. 2011) to assess for variable tuning of muscle and spring stiffness and energy storage capacity. We found that species differed in their capabilities to store energy, and more specifically that Cuban tree frogs could store more energy because their muscle and spring were tuned for high energy storage.

Thus, our findings support our hypothesis that species would differ in energy storage capabilities. Yet, our findings do not fully resolve the observations of Roberts et al. (2011) which showed that three species of frogs varied substantially in jumping power but not in vitro muscle power. This is largely because in our study we only examine the work that was stored as potential energy. In ideal systems with Hookean springs and instantaneous-release latches we could be certain that the energy stored would equal the energy that was returned. However, biological springs are non-Hookean and can lose up to 10% of stored energy as heat to the environment (Ker 1981). Furthermore, studies show that energy can be lost to latches that do not release instantaneously (Ilton et al. 2018; Divi et al. 2020). The anuran latch is a geometric-release latch that arises through dynamic changes in the muscle's mechanical advantage (Astley and Roberts 2014; Olberding et al. 2019). As such the release of energy is not instantaneous and therefore subject to losses during unlatching (Astley and Roberts 2014; Abbott et al. 2019; Divi 2020). These components of the jumping mechanism in anurans are sites where additional variation could be introduced into the system resulting in even larger discrepancies than what we would expect based on energy inputs. Quantifying how the latching (and unlatching) mechanics of the anuran system mediates energy release is an important next step to resolving the observations that there is substantial variation in anuran jumping power (Roberts et al. 2011; Astley 2016; Mendoza et al. 2020). Variation in anuran jumping power likely also arises because anurans use both spring recoil and direct muscle contributions to actuate jumps (Azizi and Roberts 2010; Astley and Roberts 2012; Sutton et al. 2019). Azizi and Roberts (2010) showed that the *plantaris longus* continues to shorten during limb extension (after storing energy in springs) suggesting that the muscle is contributing work in addition to what is being returned by recoiling springs. Future studies should examine how much work these muscles are contributing

to the jump in addition to spring recoil during limb extension, and whether these contributions can explain some of the variation in jumping power that we examine across species.

Several scaling studies have suggested that the use of elastic mechanisms for ballistic movements like jumping is most beneficial at smaller sizes (Ilton et al. 2018; Sutton et al. 2019; Mendoza et al. 2020). This reliance is largely due to the force-velocity tradeoff of muscles, which dictates that a muscle can either contract slowly and forcefully or it can contract quickly and generate low forces. This property becomes very limiting at small scales (Sutton et al. 2019) because small jumpers need to be able to generate substantial power outputs with little time to maintain jump performances that are comparable to larger jumpers (Ilton et al. 2018; Biewener and Patek 2018; Sutton et al. 2019; Mendoza et al. 2020). Small jumpers are able to circumvent these limitations by loading energy into elastic structures through slow and forceful contractions and then releasing this energy to actuate movement. In this study we found that the *plantaris longus* in Cuban tree frogs could generate more force per unit muscle mass, and that they had relatively stiffer elastic elements than bullfrogs and cane toads suggesting that the *plantaris longus* MTU of Cuban tree frogs was modified for high energy storage. Here we found that the *plantaris longus* of Cuban tree frogs could store mass-specific energies averaging 53 $J/kg_{muscle\ mass}$ (range: 32 - 81 $J/kg_{muscle\ mass}$). Olberding and Deban's (2018) intraspecific scaling study showed that the *plantaris longus* of Cuban tree frogs could generate mass-specific energies up to 73 $J/kg_{muscle\ mass}$, which falls within the range that we measured, and was approximately two times greater than that of the other species measured (average 20 $J/kg_{muscle\ mass}$ for the cane toad and 36 $J/kg_{muscle\ mass}$ for the bullfrog). Cuban tree frogs' impressive energy storage capabilities are likely necessary to provide sufficient mechanical energy within the short timescale available achieve jump takeoff. In contrast, larger jumpers (e.g. like bullfrogs and cane toads) may not

necessitate high energy storage capabilities because they have more time to takeoff (Biewener and Patek 2018; Ilton et al. 2018; Sutton et al. 2019; Mendoza et al. 2020).

CONCLUSION

In conclusion, we examined the *plantaris longus* MTU's capacity to store energy across three frog species. We found that Cuban tree frogs were able to store an impressive amount of energy because they had muscles that were modified to generate high mass-specific forces and elastic structures that were tuned to the high force capacity of these muscles. Furthermore, our study showed that the Cuban tree frogs modified muscle force through changes in muscle architecture. As this study focused exclusively on energy storage, future studies should investigate how the unlatching mechanics of the anuran jumping mechanism influences elastic energy return and overall jumping performance. Finally, future studies should quantify how much the hind limb musculature contributes to the anuran jump during hind limb extension as this may be an important source of performance variation. Together these studies will help us understand how shifts in the properties of LaMSA components drive variation in performance.

Table 1.1: Comparison of species *plantaris longus* muscle morphology (means ± s.e.m.).

Species	Body mass (g)	*Plantaris longus (PL)* muscle mass (g)	Fiber length (mm)	Pennation angle (°)	PCSA (cm^2)	% PL muscle mass
Cuban tree frog (*Osteopilus septentrionalis*) (n = 4)	28.48 ± 2.49	0.31 ± 0.01	7.76 ± 0.30	24.84 ± 0.14	0.34 ± 0.02	1.10 ± 0.08
Bullfrog (*Rana catesbeiana)* (n = 6)	99.62 ± 8.28	1.29 ± 0.12	13.84 ± 0.86	21.13 ± 1.06	0.82 ± 0.05	1.30 ± 0.06
Cane toad (*Bufo marina*) (n = 8)	89.50 ± 9.40	0.97 ± 0.10	13.87 ± 0.70	19.75 ± 1.24	0.61 ± 0.03	1.10 ± 0.06

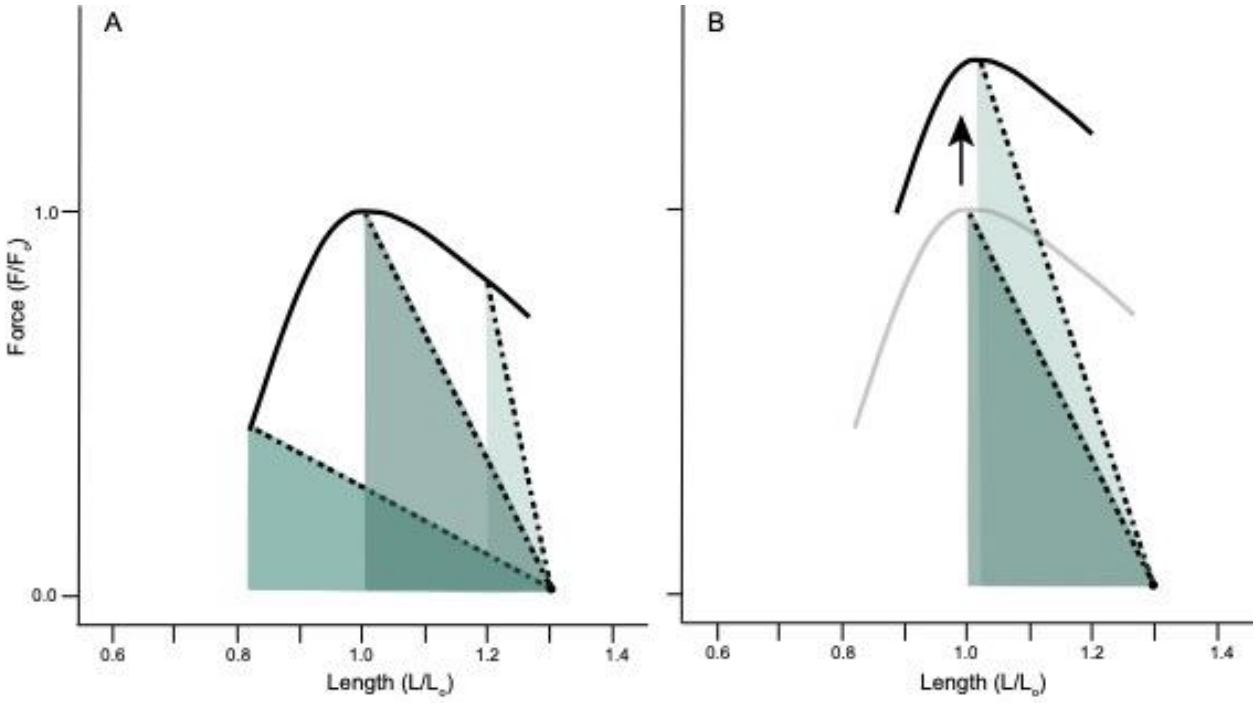

Figure 1.1: Conceptual figures showing the how the relative properties of muscles and springs can affect the amount elastic energy storage. A series of contractions are shown which all begin at a length of 1.3 L_o and shortens against the stretch of a tendon until the contraction reaches a point on the isometric force-length relationship. The slope of the dashed lines indicate spring stiffness, and the area underneath the dashed lines corresponds to the energy stored. (A) A muscle that contracts against relatively stiff elastic structures (right) could store approximately 27% of the maximal energy it could store with tuned springs. A muscle that contracts against relatively compliant elastic structures (left) would store approximately 72% of the maximal energy. Thus, tuning spring stiffness to muscle force capacity should maximize energy storage. (B) The force-length relationship shifted upward for a muscle modified for increased force capacity. With a higher force capacity a relatively stiffer spring should maximize energy storage.

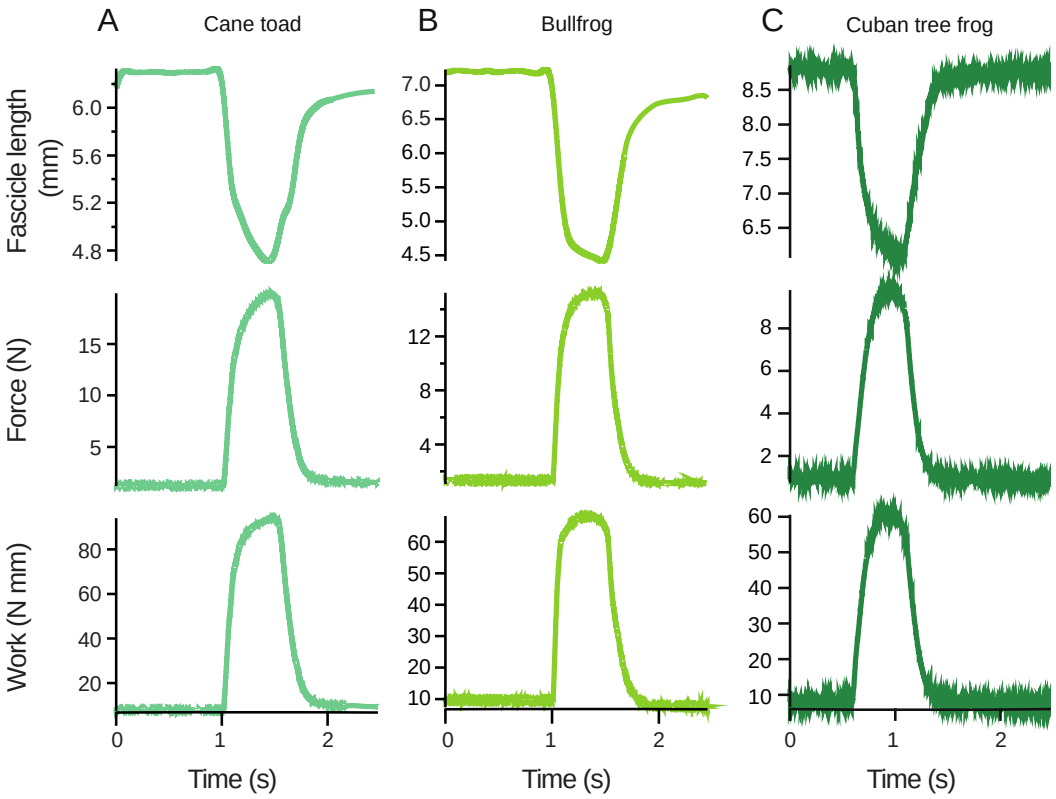

Figure 1.2: Sample time series of fixed end contractions showing fascicle length, force, and work for A) cane toad, B) bullfrog, and C) Cuban tree frog.

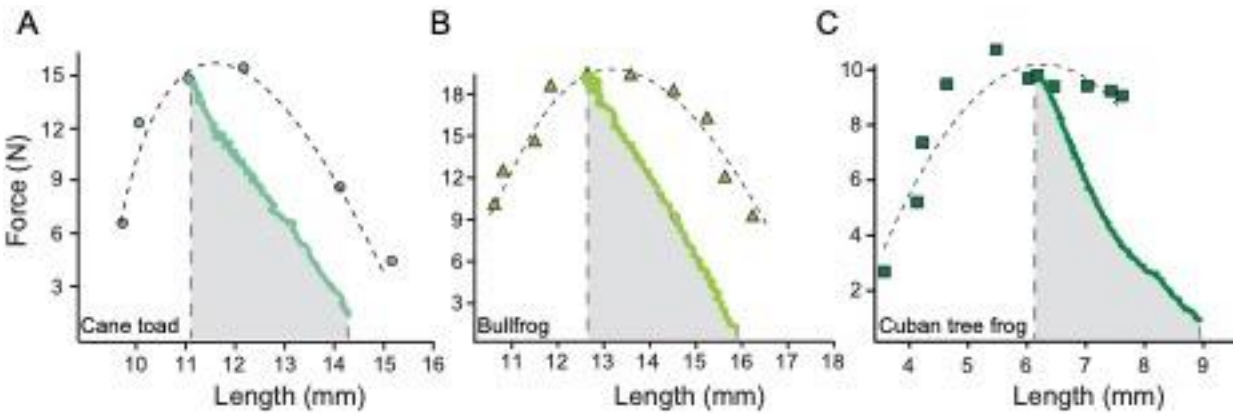

Figure 1.3: Representative force-length curves for A) Cuban tree frogs, B) cane toads, and C) bullfrogs. One representative contraction that produced the highest work is shown for each species. The muscles start at on the descending limb of the F-L curve and shorten onto the plateau against the stretch of the tendon. The shaded triangles represent the work (or energy) that was stored into the elastic elements.

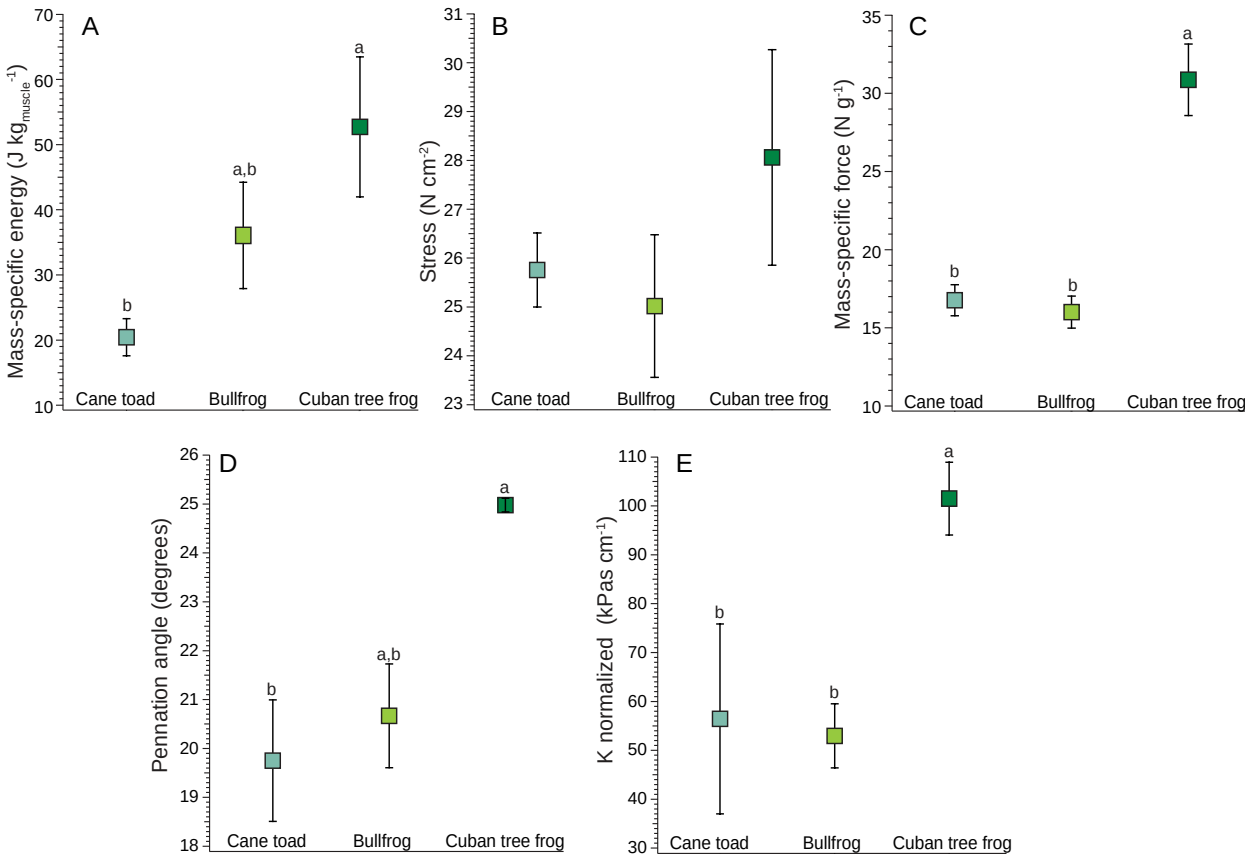

Figure 1.4: Summary data plots for A) mass-specific elastic energy, B) muscle stress, C) mass-specific force, D) pennation angle, and E) normalized stiffness. Mass-specific energy was significantly different between Cuban tree frogs and cane toads ($p<0.05$). Stress did not significantly differ across species. Mass-specific force was significantly different between Cuban tree frogs and cane toads ($p<0.001$) and between Cuban tree frogs and bullfrogs ($p<0.001$), but was not significantly different between cane toads and bullfrogs. Pennation angle was significantly different between Cuban tree frogs and cane toads ($p<0.05$). Normalized stiffness was significantly different between Cuban tree frogs and cane toads ($p<0.05$) and between Cuban tree frogs and bullfrogs ($p<0.05$), but was not significantly different between cane toads and bullfrogs.

CHAPTER 2:

Temperature effects on elastic energy storage and release in a system with a dynamic mechanical advantage latch

INTRODUCTION

Many physiological processes are sensitive to changes in temperature (Bennett 1984; Bennett 1985; Bennett 1990; Angilletta et al. 2002; James 2013). This can pose a challenge to ectothermic organisms that rely on environmental conditions to regulate body temperature and physiological rates. In animal locomotion, sprint speed in lizards, jump distance and swim speed in frogs have been shown to be sensitive to changes in temperature (Bennett 1990; Hertz et al. 1982; Herrel et al. 2007; Navas 1996; Peplowski and Marsh 1997; Navas et al. 1999). These temperature dependent changes in locomotor performance are linked to the strong thermal sensitivity of muscle contractile kinetics (e.g., shortening velocity, rate of force development, and power), and can have consequences for organism survival (Hertz et al. 1982; Putnam and Bennett 1982; Bennett 1984; Lutz and Rome 1996; Peplowski and Marsh 1997; James 2013).

Temperature coefficients (Q_{10}) are often used to indicate the rate of change of a variable when temperature is increased by 10°C. A Q_{10} equal to 1.0 indicates that the variable measured does not change much over the range of temperatures measured. A Q_{10} equal to 2.0 indicates that the variable measured increases by two-fold over the range of temperatures measured. A Q_{10} equal to 0.5 indicates that the variable measured is halved over the range of temperatures measured (Bennett 1984; Lutz and Rome 1996; Peplowski and Marsh 1997; James 2013). In animal locomotion, Q_{10} have been used to compare performance metrics of movements to the

performance of underlying muscle across temperature ranges to understand whether temperatures effects on muscle limit locomotion (Else and Bennett 1987; Swoap et al. 1993; Johnson et al. 1996; Peplowski and Marsh 1997; Navas et al. 1999; Olberding and Deban 2021).

Some ectothermic organisms use elastic recoil mechanisms to perform high-powered movements that are more robust to changes in temperature than what would be expected based on the Q_{10} of muscle alone (James 2013; Olberding and Deban 2021). Muscle contractile velocity, rate of force development or yank (Lin et al. 2019), and power show Q_{10} values that range between 1.5 - 3.0 (Putnam and Bennett 1982; Bennett 1984; Rome 1990; Peplowski and Marsh 1997) indicating that with a 10°C change in temperature there is a two-to-three-fold increase in rate. In contrast, peak velocity, acceleration, and power of elastically actuated tongue projection in chameleons shows Q_{10} values that range from 1.1-1.3 across 15-25°C indicating that tongue projection is relatively insensitive to the change in temperature (Anderson and Deban 2010). Thermal robustness through elastic recoil has also been observed in salamander tongue projection (Deban and Richardson 2011; Scales et al. 2017; Deban et al. 2021) and frog and toad tongue projection and ballistic mouth opening (Deban and Lappin 2011; Sandusky and Deban 2012) suggesting that elastic recoil mechanisms underlie thermally robust behaviors in some ectothermic organisms.

Elastic recoil mechanisms drive some of the fastest and most powerful movements ever recorded in biology (Ilton et al. 2018; Longo et al. 2019; Longo et al. 2021). In animals, these extremely fast and powerful behaviors are the result of finely tuned interactions between muscle, spring (e.g., tendon, aponeurosis, apodeme), latch, and projectile (Ilton et al. 2018; Longo et al. 2019). When the latch becomes engaged this allows for decoupling of muscle contraction from joint motion and for muscle to contract and store energy in surrounding springs. Latch removal

initiates the rapid release of energy by the spring (Ilton et al. 2018; Longo et al. 2019; Divi et al. 2020). Energy released by the spring actuates the projectile and results in extremely high-powered motion (Ilton et al. 2018; Longo et al. 2019; Divi et al. 2020). In some cases, spring actuation also results in thermally robust movements (Anderson and Deban 2010; Deban and Richardson 2011; Deban and Lappin 2011; Sandusky and Deban 2012; Scales et al. 2017; Deban et al. 2021).

Recent work examining the role of the latch in mediating energy flow has shown that the latch substantially influences elastic recoil performance (Ilton et al. 2018; Abbott et al. 2019; Divi et al. 2020). Previous modeling studies have shown that the amount of energy returned decreased with relatively slower latch removal velocities indicating that the elastic recoil mechanism is sensitive to latch behavior (Ilton et al. 2018; Abbott et al. 2019; Divi et al. 2020; Acharya et al. 2021). However, it is not yet understood whether external factors like temperature can affect latch performance and how changes to latch dynamics may allow for the contribution of direct muscle power to actuate the system.

Frog jumps are one of the most well-studied examples of elastically actuated movements (Marsh 1994; Peplowski and Marsh 1997; Roberts and Marsh 2003; Azizi and Roberts 2010; Astley and Roberts 2012; Astley and Roberts 2014; Astley 2016; Mendoza et al. 2020). Previous studies have shown decoupling of muscle contraction from joint movement as evidence of elastic energy storage at the ankle joint (Roberts and Marsh 2003; Azizi and Roberts 2010; Astley and Roberts 2012). The elastic recoil mechanism in frog jumps is mediated by a dynamic mechanical advantage latch, where the poor mechanical advantage of the hind limb extensor muscles and the body's inertia serve as a latch that resists hind limb joint extension early in the jump and allows for energy storage. Once the hind limb extensor muscles build sufficient force to overcome the

latch, the hind limb joints begin to extend, and the mechanical advantage of the extensor muscles improves simultaneously (Roberts and Marsh 2003; Olberding et al. 2019; Astley and Roberts 2014). Results from previous studies provide some evidence that the muscle may continue to shorten as the tendon recoils providing some evidence that this latching mechanism allows for a combination of elastic and direct muscle energy to contribute to jumps (Roberts and Marsh 2003; Azizi and Roberts 2010; Astley and Roberts 2012; Sutton et al. 2019).

Despite the use of elastic mechanisms, frog jumping performance remains temperature sensitive (Hirano and Rome 1984; John-Alder et al. 1988; Whitehead et al. 1989; Rome 1990; Marsh 1994; Peplowski and Marsh 1997; Navas et al. 1999; Olberding and Deban 2021). For example, Hirano and Rome (1984) showed that jump power operated with Q_{10} of 2.67, jump velocity with a Q_{10} of 3.33, and jump distance with a Q_{10} of 1.58 between 15-25°C in the leopard frog (*Rana pipiens*). In this study we investigate how the latching mechanics of the frog jump mechanism affects their ability to store and release energy across temperature. Here we aim to reveal the mechanism that causes frog jumps to be temperature dependent and to determine whether the observed thermal sensitivity is due to differences in energy storage or release. We used an *in vitro* muscle preparation coupled with an *in silico* model of a jumper because it allowed us to control muscle performance through direct stimulation, while allowing our muscles to interact with realistic movement dynamics. We hypothesized that the amount of energy stored (i.e., work) would not change with temperature since slowing muscle contractions would only increase the duration and not the amount of elastic energy storage. Additionally, muscle contractile rates are sensitive to temperature thus, we hypothesized that the amount of energy released (i.e., work) would be temperature dependent because of the additional work that may be contributed by extensor muscles during elastic recoil and joint extension (Bennett 1984; Bennett

1985; Rall and Woledge 1989; Roberts and Marsh 2003; Azizi and Roberts 2010; Astley and Roberts 2012).

MATERIALS AND METHODS

Animals

Six similarly sized (mean ± standard error of the mean; mass = 100.25 ± 4.23g) bullfrogs (*Rana catesbeiana*) were purchased from a herpetological vendor, Rana Ranch (Idaho, USA). The animals were group housed in glass terraria and were fed calcium-enriched crickets *ad libitum*. Animal husbandry and use were approved by the University of California, Irvine Animal Care and Use Committee (protocol AUP 20-129).

Muscle preparation

In this study, we followed methods outlined by Azizi and Roberts (2014) and Mendoza and Azizi (2021). Briefly, frogs were euthanized with a double pithing protocol. Once death was confirmed, we measured the length of the tibiofibula segment with digital calipers. We isolated the sciatic nerve branch running along the right femur. Then, we exposed the *plantaris longus* muscle and implanted a sonomicrometry crystal between two muscle fascicles near the muscle origin. A second crystal was implanted ~8mm distal to the first and both were secured with 6-0 silk. After instrumentation, we isolated the muscle preparation from the body by detaching the muscle's distal tendon from the plantar fascia and isolating the knee joint (where the muscle originates). The instrumented muscle was secured to a fixed clamp at the knee joint and the distal tendon was threaded through a custom-made clamp. The clamp on the distal tendon was attached to a 50N servomotor (Aurora Scientific Inc., Ontario, CA, USA). The sciatic nerve was threaded

through a custom-made nerve cuff that was connected to a Grass S99D stimulator (Grass Technologies, Warwick, RI, USA), and was used to electrically stimulate the muscle. Finally, the muscle preparation was placed in a bath of circulating anuran ringer's solution maintained at room temperature (e.g. 20°C) with a temperature controller circulator. The bath was continuously aerated with oxygen.

Muscle property characterization

Optimal stimulation voltage was determined by twitch contractions. For each muscle we determined optimal stimulation voltage by increasing the voltage of twitch contractions by one-volt increments until force stopped increasing with increasing voltage (9–11V). Next, we determined optimal muscle length (L_o) by characterizing the force-length curve using tetanic fixed-end contractions at variable lengths. L_o was defined as the length at which the muscle produced the highest peak force (P_o). Muscle fascicle length changes were measured with sonomicrometry, and muscle force and muscle-tendon unit (MTU) length were measured with the servomotor. Tetanic stimulation consisted of 0.2ms pulses at 65 pulses per second and durations of 500ms. Once L_o was determined, muscles were set to L_o for all experimental contractions.

Experimental set-up and mechanical advantage latch parameters

To investigate the temperature effects on energy flow in a system with a dynamic mechanical advantage latch, we developed a novel *in vitro in silico* muscle preparation. Specifically, our isolated muscle preparation interfaced with a BeagleBone Black computer with real-time feedback control that was programmed with Olberding et al. (2019)'s virtual jumper

(Fig. 2.1A). Briefly, the modeled jumper consisted of two massless and frictionless segments that came together to form a first-class lever. In the model, a muscle is positioned parallel to the upper segment, and it applies input force (F_m) at the end of the in-lever (L_i). Force applied by the muscle acts through the mechanical advantage of the joint and exerts a ground reaction force that accelerates a gravitational mass positioned at the end of the upper segment (see Olberding et al. 2019 for more details). For our experiments, we modified Olberding et al. (2019)'s jumper as follows: segment length was set equal to the length of the right tibiofibula measured for each individual frog (n = 6; mean ± se; tibiofibular length = 34.84 ± 0.70mm). We replaced the muscle in the model with an *in vitro* muscle preparation of the *plantaris longus* MTU and the force generated by the muscle F_m was fed into the model. Projectile mass, P_{mass}, was scaled based on muscle mass to body mass ratios from Marsh (1994) and Olson and Marsh (1998).

$$P_{mass} = \text{Muscle mass}_{estimated}/0.17 \quad (1)$$

We calculated in-lever length, L_{in}, based on the mechanical advantage, *MA*, required to overcome the gravitational load of the mass and inertia given a peak force of $0.6P_o$ and a starting joint angle of 10° (see Table 2.1). Because of the slight decrease in force due to changes in temperature we chose $0.6P_o$ to ensure that the muscles would consistently overcome the force threshold (Olberding and Deban 2017). We acknowledge that Olberding et al. (2019)'s model contains a calcaneus, and that frogs do not possess this anatomical structure. Again, the goal of the model is not to mimic a frog's anatomy or behavior, but rather to provide us a controlled framework to compare patterns of energy flow through a system with a MA latch across a range of temperatures.

Temperature manipulations

After characterizing the force-length relationship, we ran the *in vitro in silico* experiments across four temperature treatments: 10, 15, 20, and 25°C. All experiments started with 20°C and were followed by either sequence 10-15-25-20°C or 25-15-10-20°C. We ran the temperature experiments in this fashion to minimize the potential confounding interactions between muscle fatigue and temperature. The temperature of the circulating ringer's solution was manipulated with a temperature controller, and we monitored the solution's temperature with a temperature probe. Once the ringer's solution reached treatment temperature, we waited 20 minutes to allow the muscle to reach the experimental temperature (Olberding and Deban 2017). Then the muscle was lengthened to L_o, the model and the reactive feedback control loop was initiated, and the muscle was stimulated tetanically as describe above. The details of the real-time feedback controller were previously described in detail by Reynaga et al. (2019). Briefly, the servomotor registered the force generated by the muscle and broadcasted the analog signals in the ±10V range. A peripheral 16-bit sampling analog-to-digital (A/D) unit on the custom printed circuit board converted this signal to a digital force measurement, which was then passed via the serial peripheral interface bus to the BeagleBone, where it was smoothed with a software-implemented low-pass filter (Reynaga et al. 2019). The smoothed force and starting MA were used to calculate the displacement of the projectile's center of mass. The digital displacement value was then passed from the BeagleBone to a peripheral 16-bit multiplying digital-to-analog converter chip, where it was converted to an analog control signal. The analog control signal was sent to the servomotor, which controlled the position of the muscle lever (MTU length; Fig. 1A). This feedback loop continued until the muscle reached the force threshold. Once the muscle generated sufficient force to overcome the force threshold the modeled joint began to extend and

accelerate the mass. Experiments ended when joint angle reached 180° or when force was equal to zero.

After experimentation, the muscle was detached from its origin at the knee joint and the distal free tendon was removed. Muscle mass, fascicle length, and pennation angle were measured and used to calculate muscle stress using a known muscle density of 1.06 g cm^{-2} (Mendez and Keys 1960). Muscle stress was calculated to ensure that the muscle preparations were of good quality (i.e., within physiological range ~20 N cm^{-2}; Table 2.1) (Roberts et al. 2011; Mendoza and Azizi 2021).

Data processing

All data were processed in Igor Pro software (Wavemetrics, Lake Oswego, OR, USA). To interrogate the role of a dynamic mechanical advantage latch in mediating energy flow we partitioned our data into two phases, the loading and unloading phase (Fig. 2.1B). In the loading phase the latch was engaged and resisted motion, which allowed the muscle fascicles to contract and store energy into elastic elements. Because the latch was engaged the MTU maintained a constant length, so any shortening of the muscle fascicles would result in an equal stretch of the elastic elements. In these experiments we defined the 'loading phase' as the start of muscle force development until peak muscle force. We measured loading muscle fascicle work (i.e., energy stored) by plotting muscle fascicle length against muscle force during the loading phase and calculating the area under this curve.

In the unloading phase, the latch was removed, and this allowed the elastic elements to recoil while the muscle fascicles continued to do work during joint extension, simultaneously. We defined the 'unloading phase' as starting from peak muscle force to when muscle force was

equal to zero (Fig. 2.1B). We measured the work done by muscle fascicles during joint extension (i.e., unloading muscle fascicle work) by plotting muscle fascicle length and muscle force during the unloading phase and calculating the area under this curve.

We interrogated the unloading phase further by parsing out the relative contributions of tendon recoil work and direct muscle fascicle work (i.e., during joint extension). To do this, we measured total MTU work by plotting muscle force against MTU length during the unloading phase. The area under this curve was the total MTU work done during the unloading phase. To calculate tendon recoil work, we subtracted unloading muscle fascicle work from total MTU work. All measurements of work were converted to muscle-mass-specific work by dividing by *plantaris longus* muscle mass.

We calculated efficiency, by taking the ratio of tendon recoil work to loading muscle fascicle work. Additionally, we calculated the relative contributions of direct muscle fascicle work and tendon recoil work during joint extension. We calculated this by taking the ratio of tendon recoil work to unloading muscle fascicle work. Lastly, we measured the duration of both the loading and unloading phase. We used this to calculate muscle fascicle power and tendon power.

Analyses

All statistical analyses were performed in R (http://www.R-project.org/). We performed linear mixed models that included temperature as the continuous variable and individuals as a random factor (Olberding and Deban 2017; Olberding et al. 2018). For this analysis we used the function *lme* in the R package *nmle* (version 3.1). All dependent variables except for durations were log-transformed because their relationships were expected to be exponential with

temperature. Dependent variables were analyzed separately across three temperature ranges: 10-20, 10-25, and 15-25°C. We used the partial regression coefficient of temperature to calculate temperature coefficients (Q_{10}) using the equation:

$$Q_{10} = 10^{(\text{regression coefficient} \times 10)} \quad (6)$$

(Deban and Lappin 2011; Deban and Richardson 2011; Anderson and Deban 2012; Scales et al. 2017; Olberding and Deban 2017; Olberding et al. 2018). We reported Q_{10} of durations as inverse Q_{10} values (e.g. $1/Q_{10}$) to express them as rates (Deban and Lappin 2011). The p-values for the regression coefficients for all tests were adjusted using the Benjamini-Hochberg procedure to control for false discovery (Benjamini and Hochberg 1995). Temperature coefficients were significantly different from 1.0 if the p-value for the regression coefficients were less than the adjusted alpha.

RESULTS

As expected, an increase in temperature resulted in a decrease in the duration of all phases of the *in vitro in silico* experiments (Fig. 2.2 A, B, C). Loading and unloading time both decreased with increase in temperature (Fig. 2.2 B, C). Loading time was longer than unloading time. Loading time showed temperature coefficients that were significantly different from 1.0 across all three temperature ranges. Specifically, 10-20°C had a $1/Q_{10}$ of 1.51 ($p=0.002$), 15-25°C had a $1/Q_{10}$ of 1.08 ($p=0.021$), and 10-25°C had a $1/Q_{10}$ of 1.29 ($p=0.005$; Fig. 2.2B). Unloading time did not have temperature coefficients that were significantly different from 1.0 across all three temperature ranges. Specifically, temperature coefficients at temperature ranges 10-20°C was $1/Q_{10}$ =1.06 ($p=0.042$), 10-25°C was $1/Q_{10}$ =1.13 ($p=0.064$), and 15-25°C was $1/Q_{10}$=0.99 ($p=0.090$; Fig. 2.2C).

We found that peak force increased with increase in temperature and peaked at 20°C (Fig. 2.2D). The Q_{10} for peak force across 10-20°C and 10-25°C were 1.2 and 1.1, respectively, and were significantly different from a Q_{10} of 1.0 (p=0.00 and p=0.0054, respectively). The Q_{10} for the temperature range of 15-25°C was not significantly different from 1.0, p=0.488 (Fig. 2.2D).

In vitro in silico contractions produced workloops that more closely captured the dynamics experienced by the muscle during joint extension compared to a traditional tetanic fixed-end contraction (Fig. 2.3). Loading muscle work increased with increase in temperature (Fig. 2.3B, C and 2.4A). However, the Q_{10} for loading muscle work across all temperature ranges did not significantly differ from 1.0 and were 1.5 for 10-20°C (p=0.020), 1.2 for 10-25°C (p=0.068), and 1.1 for 15-25°C (p=0.295; Fig. 2.4A). Tendon recoil work increased with increase in temperature (Fig. 2.4B). The temperature range of 10-20°C had a Q_{10} of 1.5 and was significantly different from a Q_{10} of 1.0 (p=0.003). The temperature range 10-25°C and 15-25°C had Q_{10} values equal to 1.2 (p=0.072) and 1.0 (p=0.735) respectively and were not significantly different from a Q_{10} of 1.0 (Fig. 2.4B). Unloading muscle work increased significantly with increase in temperature (Fig. 2.3B, C and 2.4C). The Q_{10} for unloading muscle work across all temperature ranges significantly differed from 1.0 and were 2.2 for 10-20°C (p=0.0004), 1.7 for 10-25°C (p=0.003), and 1.4 for 15-25°C (p=0.024; Fig. 2.4C).

Loading muscle power increased with increase in temperature (Fig. 2.5A). The temperature coefficient was significantly different from 1.0 for the temperature range 10-20°C (Q_{10}=2.9, p=0.001), and for the temperature range 10-25°C (Q_{10}=1.9, p=0.004, Fig. 2.5A). The temperature coefficient was not significantly different from 1.0 for the temperature range 15-25°C (Q_{10}=1.3, p=0.095, Fig. 2.5A). Tendon recoil power increased with increase in temperature

(Fig. 2.5B). The temperature range 10-20°C had a Q_{10} of 2.1 and was significantly different from a Q_{10} of 1.0 (p=0.007, Fig. 2.5B). The temperature range of 10-25°C had a Q_{10} of 1.5 (p=0.034) and the temperature range 15-25°C had a Q_{10} of 1.0 (p=0.985) and they were not significantly different from a Q_{10} of 1.0 (Fig. 2.5B). Unloading muscle power increased with increase in temperature (Fig. 2.5C). The Q_{10} for 10-20°C was 3.1 (p=0.001), 10-25°C was 2.1 (p=0.003) and 15-25°C was 1.4 (p=0.029), and all temperature ranges were significantly different from a Q_{10} of 1.0 (Fig. 2.5C).

The tendon recoil work-to-unloading muscle work ratio did not significantly change with increase in temperature (Fig. 2.6A). Q_{10} values for the temperature ranges 10-20°C (Q_{10} =0.7; p=0.021), 10-25°C (Q_{10} =0.7; p=0.059), and 15-25°C (Q_{10} =0.7; p=0.233) were not significantly different from a Q_{10} of 1.0 (Fig. 2.6A). Efficiency did not change with temperature (Fig. 2.6B). Average efficiency was approximately (mean ± SEM) 41.17 ± 2.95% across all temperature treatments. Q_{10} values for the temperature ranges 10-20°C (Q_{10} =1.0; p=0.923), 10-25°C (Q_{10} =1.0; p=0.933), and 15-25°C (Q_{10} =0.9; p=0.553) were not significantly different from a Q_{10} of 1.0 (Fig. 2.6B).

DISCUSSION

Thermal robustness achieved through spring actuation has been demonstrated in some ectothermic organisms (Anderson and Deban 2010; Deban and Lappin 2011; Deban and Richardson 2011; Deban et al. 2020; Olberding and Deban 2021). However, it appears that the degree of insensitivity to changes in temperature varies across systems. Jumping in frogs has been shown to be relatively more sensitive to changes in temperature than other systems (e.g. chameleons) despite documented use of spring actuation (Hirano and Rome 1984; Azizi and

Roberts 2010; Astley and Roberts 2012). This suggests that the specific mechanics of LaMSA are critical for producing movements that are thermally robust. In this study we investigated how the latching mechanics mediated energy flow in a jumper with a dynamic mechanical advantage latch. We hypothesized that loading muscle fascicle work would not differ across temperature treatment because unlatching would not occur until the muscle reached the force threshold and lowering temperature would only increase the time required to reach such a threshold. Moreover, we predicted that unloading muscle fascicle work would differ across temperature treatment because of temperature effects on muscle contractile rates (Bennett 1984; Bennett 1985; Rall and Woledge 1989). We found that loading muscle fascicle work differed across temperature treatments and did not support our hypothesis (Fig. 2.4A). We found that tendon recoil work showed temperature dependence that reflected the work pattern observed during the loading phase (Fig. 2.4B). Furthermore, we found that unloading muscle fascicle work showed strong temperature dependence and this result supported our hypothesis (Fig. 2.4C). Our results suggest that a dynamic mechanical advantage latch cannot fully decouple muscle contraction from joint motion allowing for temperature effects to affect motion. Our results suggest that movements that are actuated by a combination of elastic recoil and direct muscle actuation will not display the thermal robustness observed in other LaMSA systems (Anderson and Deban 2010; Deban and Lappin 2011; Deban and Richardson 2011; Deban et al. 2020; Olberding and Deban 2021). Together, our results indicate that temporal decoupling of muscle contraction from movement is critical for thermally robust movements (e.g. like chameleon tongue projection; Wainwright and Bennett 1992; Anderson and Deban 2010).

Loading muscle fascicle work differed across temperatures although these differences were not statistically significant (Fig. 2.4A). Differences in loading muscle fascicle work were

due to the muscle fascicles contributing work after unlatching and unlatching delays introduced by the inertial latch (Fig. 2.3B, C and 2.4A). Specifically, once the muscle reached the unlatching threshold, unlatching of the geometric latch initiated. During this time, the muscle remained active and continued to shorten and generate force as the body's inertia slowed the movement of the center of mass and limited limb extension. This delay resulted in warmer (faster) muscles overshooting the force threshold more than colder muscles and continuing to store more energy than colder muscles (Fig. 2.2D, 2.3B, C). Furthermore, because there was variation in the amount of work stored during the loading phase, tendon recoil work also varied with temperature (Fig. 2.4B).

Previous studies have shown that the *plantaris longus* muscle continues to shorten during limb extension in frog jumps (Roberts and Marsh 2003; Azizi and Roberts 2010; Astley and Roberts 2012), yet the relative importance of this contribution remained unknown because *in vivo* measurements of muscle force are difficult to acquire in frogs (although see Richards and Biewener 2007 and Moo et al. 2017). In our study, we found that muscle fascicle work during the unloading phase showed strong thermal dependence across all temperature ranges (Fig. 2.4C). We found that unloading muscle fascicle work operated with Q_{10} values of 2.2, 1.4, and 1.7 across the temperature ranges of 10-20°C, 15-25°C, and 10-25°C, respectively. At the coldest treatment the muscle was able to contribute on average about 3.5 J $kg_{muscle\ mass}^{-1}$, while at its warmest temperature the muscle contributed on average approximately 8 J $kg_{muscle\ mass}^{-1}$ (Fig. 2.4C). At warmer treatments the amount of work contributed by the muscle fascicles during the unloading phase was on par with that returned by tendon recoil (Fig. 2.4B, C and Fig. 2.6A). Furthermore, as temperature decreased the relative contribution of muscle work decreased (although statistically it was not significantly different), and tendon recoil work contributed

relatively more work to the jump (Fig. 2.4B, C and Fig. 2.6A). Our results showed that the work contributions of muscle during the unloading phase are as important as those of tendon recoil and highlight the hybrid nature of this jump mechanism (Sutton et al. 2019; Olberding et al. 2019).

The unlatching mechanics affected efficiency and introduced thermal sensitivity. In our experiments, we found that elastic recoil operated with an average efficiency of 41.2% across all temperatures (Fig. 2.6B). Efficiency is substantially lower than previous reports of approximately 90% efficiency in tendon when measured during relatively slow cyclical tensile conditions (Ker 1981). This low efficiency is likely due to energy dissipation during unlatching. Abbott et al. (2019) modeled an elastic recoil system with an antagonist muscle as a latch and showed that unlatching velocity (i.e., muscle relaxation rate) was critical for determining whether power would be amplified or attenuated. They found that the fastest unlatching resulted in substantial power amplification and the slowest unlatching resulted in power attenuation. Furthermore, Divi et al. (2020) modeled latches with different latch removal velocities and showed that slower unlatching resulted in increased control of projectile launch at the cost of efficiency. While our study does not examine unlatching velocity our estimates of efficiency suggest that there may be an emphasis on control of jump trajectory during actuation that may result in a tradeoff with efficiency. The studies mentioned above support our findings and collectively suggest that unlatching duration may serve as a form of control on output performance at the incurred cost of energy loss (Hyun et al. 2023). Furthermore, although integration of the two phases resulted in temperature sensitive movements, it may be of importance for control. In the frog jumping mechanism muscles loaded work into elastic elements while the latch was engaged and continued to do work during unlatching and limb extension. Continuous contribution of work by the muscle throughout the jump suggests that

frogs may have the ability to control the performance and directionality of the jump after unlatching. The ability to control a movement in real time after unlatching would likely not be possible in organisms where the muscle only contributes energy during energy storage, and where the latch temporally decouples energy storage from energy return (Roberts 2019). Thus, latches like the anuran latch may result in reduced efficiency and robustness to environmental perturbations (e.g. temperature), but they afford the organism greater control of energy release and movement during the actuation phase.

Thermal robustness through elastic recoil is observed in chameleon and salamander tongue projection, and ballistic mouth opening in frogs and toads, but less so in frog or house cricket jumping (Hirano and Rome 1984; Anderson and Deban 2010; Deban and Richardson 2011; Deban and Lappin 2011; Scales et al. 2017; Olberding and Deban 2021; Deban and Anderson 2021). Deban and Anderson (2021) showed that jumping performance in house crickets was relatively more temperature sensitive than jumping in fleas and other insects despite use of elastic recoil mechanisms. The authors suggest that this could be due to additional muscle contributions during the takeoff phase, or dealing with high loads, which are known to result in temperature dependent work outputs (Olberding and Deban 2017). In our study, the required MA to overcome the latch was calculated with peak muscle force equal to $0.6P_0$ to reduce the load experienced by the muscle and fatigue, therefore it is not likely that there was an interaction effect of high load and temperature. In our study, continuous contribution of work by the muscle fascicles and the unlatching mechanics resulted in the integration of the loading and unloading phases. This continuity between the two phases allowed for transmission of muscle's thermal sensitivity into the energy stored and energy returned by elastic structures. The strongest temperature effects were observed during the unloading phase where the muscle contributed

work during joint extension. Thus, while frog jump performance is relatively more insensitive to changes in temperature than underlying muscle contractile properties, frog jump performance is relatively more sensitive to changes in temperature than other thermally robust systems (e.g. chameleon tongue projection). Our work suggests that organisms that use elastic recoil mechanisms will perform thermally independent movements only when the latch temporally decouples muscle contraction from energy release (i.e., no additional contribution by the muscle during actuation).

Among the many LaMSA systems studied to date, no system has shown a capacity to augment spring actuation with additional muscular work after the spring actuation has begun. While at first glance it would seem favorable for systems to augment mechanical energy output during the actuation phase by continuing to generate muscle work, this "hybrid" actuation operates with some important constraints. It is likely that the duration of the take-off phase of a jumping frog is largely determined by the rate of energy release by tendons constraining the time available for muscle contributions. This would suggest that the power output of the muscle must remain high enough to contribute a substantial amount of mechanical work during a limited period of time. Therefore, it is reasonable to assume that some of the fastest LaMSA systems operating with a more idealized latch simply do not provide muscles enough time to contribute significantly once unlatching has occurred (Divi et al. 2020). This would suggest that in systems using hybrid actuation, maintenance of muscle power may be favored by natural selection whereas idealized systems may move to muscles specialized for high force production (Longo et al. 2019).

Study limitations

In this study we examined the effects of temperature on elastic energy storage and return in a system with a dynamic mechanical advantage latch. We found that continuous muscle contributions and the unlatching mechanics in this system allowed for integration of energy storage and energy release that resulted in temperature dependence. While the results here demonstrate the role of unlatching mechanics in mediating energy flow there are limitations to our approach. First, we used an isolated muscle preparation coupled to a model of a jumper (Olberding et al. 2019) to understand the effects of temperature on an elastic recoil system with a dynamic mechanical advantage latch. We used limb morphology and muscle mass to scale the jumper model to each frog. Our approach assumes that the muscle physiology of the *plantaris longus* is representative of hip and other hind limb extensor muscles. The *plantaris longus* is a biarticulate muscle that flexes the knee and primarily extends the ankle (Olson and Marsh 1998). It has bipennate architecture and in bullfrogs it has a large aponeurosis sheet wrapping around the muscle belly, which is distinct from some of the hip and hind limb muscles. Yet, previous studies examining the properties of the *plantaris longus* muscle suggest that its contractile behavior may be consistent with other hind limb muscles involved in jumping. For example, Astley (2016) and Mendoza et al. (2020) showed that the underlying muscle properties of the *plantaris longus* and *semimembranosus* (parallel fibered hip extensor and knee flexor) are similar across several species of frogs from diverse microhabitats. Additionally, Deban and Lappin (2011) and Olberding et al. (2018) showed that the contractile properties of muscles used in elastic recoil mechanisms are consistent with that of typical skeletal muscle. Furthermore, *in vivo* studies in jumping bullfrogs showed that several muscles spanning the hip and hind limb showed similar activation patterns to the *plantaris longus* during jump takeoff suggesting that they have similar functional roles during a jump (Olson and Marsh 1998). Another limitation to our

approach is that we simplified neural control to supramaximal stimulation, which is known to be rare in animal locomotion (Astley et al. 2013). Future studies are necessary to understand whether the patterns observed here reflect *in vivo* patterns in frog jumps at variable temperatures. The patterns observed in our study are confounded by the limitations outlined above, yet they provide testable hypotheses for future studies examining the temperature effects on elastic energy storage and return in frog jumping *in vivo*.

CONCLUSIONS

Frog jumping performance is known to be relatively more sensitive to changes in temperature than other movements driven by elastic recoil. In this study we investigated what aspects of the jump mechanism contributed to temperature sensitivity by examining the role of latching mechanics in mediating energy storage and release. We found that continuous muscle contributions and the mechanics of a dynamic mechanical advantage latch resulted in thermal sensitivity of energy storage and energy return. Furthermore, we found that hind limb muscle plays a substantial role in actuating jumps in addition to the recoil of elastic structures. Finally, we propose that actuation through elastic recoil and direct muscle contributions results in some thermal sensitivity but allows for greater control and modulation of the jump in real time.

Table 2.1: Animal morphology and mechanical advantage parameters for the virtual joint.

Morphology				Joint Mechanical Advantage								
ID	Animal mass (g)	Muscle mass (g)	Stress (N/cm^2)	Out-lever, L_{out} (mm)	In-lever length, L_{in} (m)	Projectile mass, P_{mass} (kg)	Force threshold (N)	60 % P_o (N)	Mechanical advantage (r/R)	Muscle moment arm, r (m)	GRF moment arm, R (m)	Starting joint angle (rad)
A	112.49	1.50	24.90	34	0.0016	0.0094	11.13	10.77	0.008	0.0002778	0.033	0.174533
B	105.76	1.85	26.38	38	0.0015	0.0088	12.44	12.43	0.007	0.0002605	0.037	0.174533
C	86.48	1.28	26.03	34	0.00078	0.0047	11.41	11.33	0.004	0.0001354	0.033	0.174533
D	94.8	1.39	25.57	35	0.0011	0.0071	12.50	11.52	0.006	0.0001910	0.034	0.174533
E	109.06	1.41	24.81	33	0.0013	0.0088	12.46	12.05	0.007	0.0002257	0.032	0.174533
F	92.91	1.43	22.60	35	0.0012	0.0071	11.45	11.44	0.006	0.0002084	0.034	0.174533

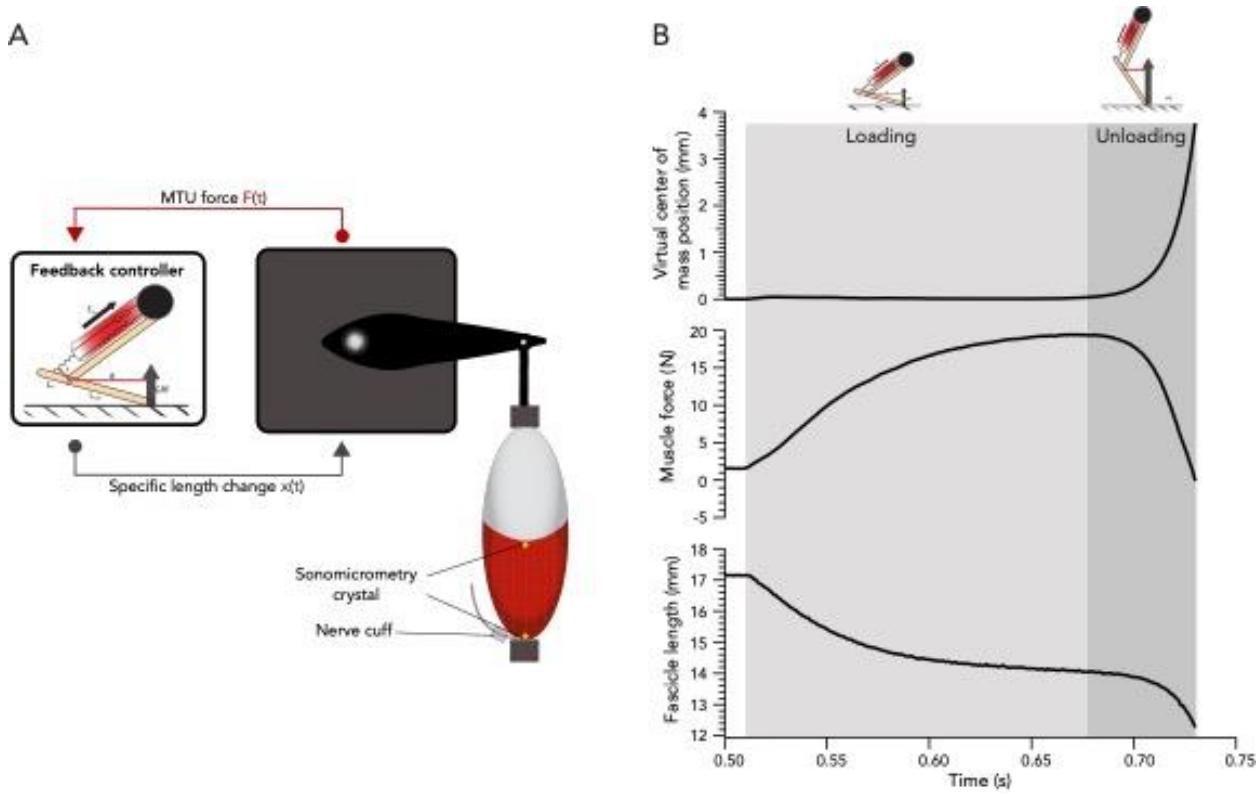

Figure 2.1: Experimental set-up. A) An *in-vitro* muscle preparation was coupled with a real-time feedback controller programmed with a model of a virtual jumper from Olberding et al. (2019). To initiate the experiment, we set the muscle to Lo, ran the model, and stimulated the muscle through a branch of the sciatic nerve. The servomotor read muscle force, and muscle force inputs were fed to the model by the servomotor. In response, the model outputted a calculated relative length change to the servomotor based on the muscle's mechanical advantage. The joint began to extend when the muscle developed sufficient force to overcome the force threshold set by gravity acting through the mechanical advantage of the joint. The experiment ended when the joint extended to 180° or when force was equal to zero. Experiments were run at four temperatures: 10, 15, 20, and 25°C. B) Example time series showing virtual center of mass position, muscle force, and muscle fascicle length at 20°C. The light grey shading indicates the loading period, and the dark grey shading indicates the unloading period.

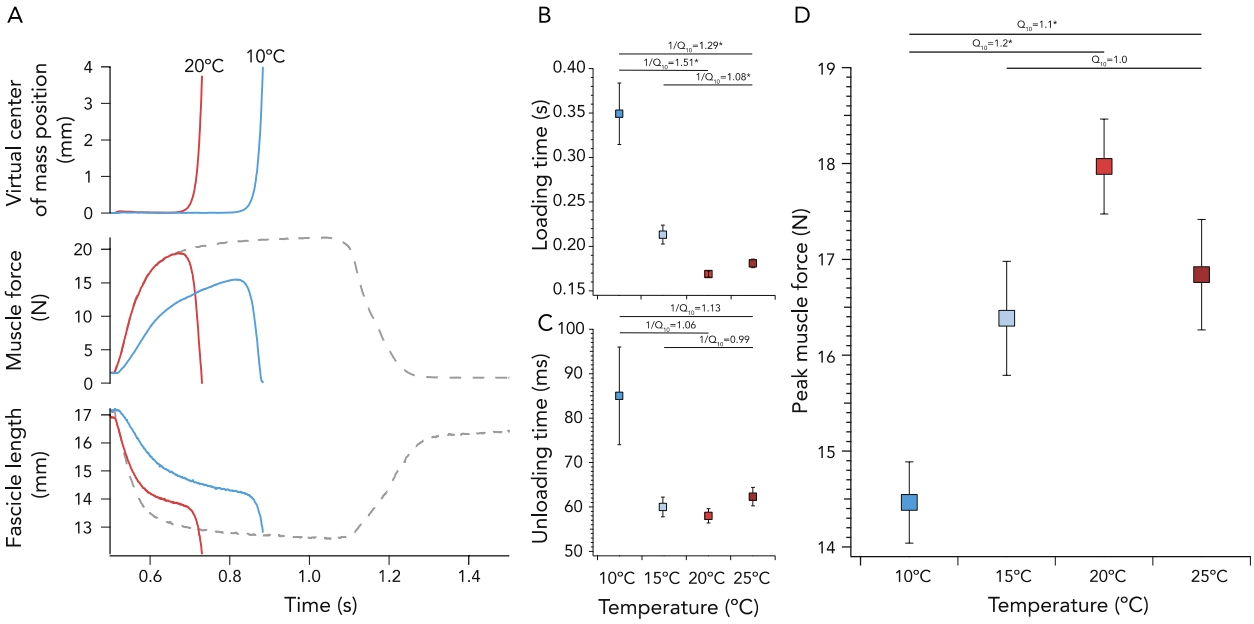

Figure 2.2: Temperature effects on durations and muscle force. A) Example time series for experiments at 10 and 20°C showing virtual center of mass position, muscle force, and muscle fascicle length. For comparison an isometric tetanic fixed end contraction is shown as grey dashed lines. Note that if the muscle could not reach the force threshold the contraction would proceed as an isometric tetanic fixed end contraction. Summary plots of B) loading time, C) unloading time, and D) peak muscle force plotted against temperature. Boxes are means and the error bars are S.E.M. Temperature coefficients significantly different from 1.0 are indicated with an asterisk.

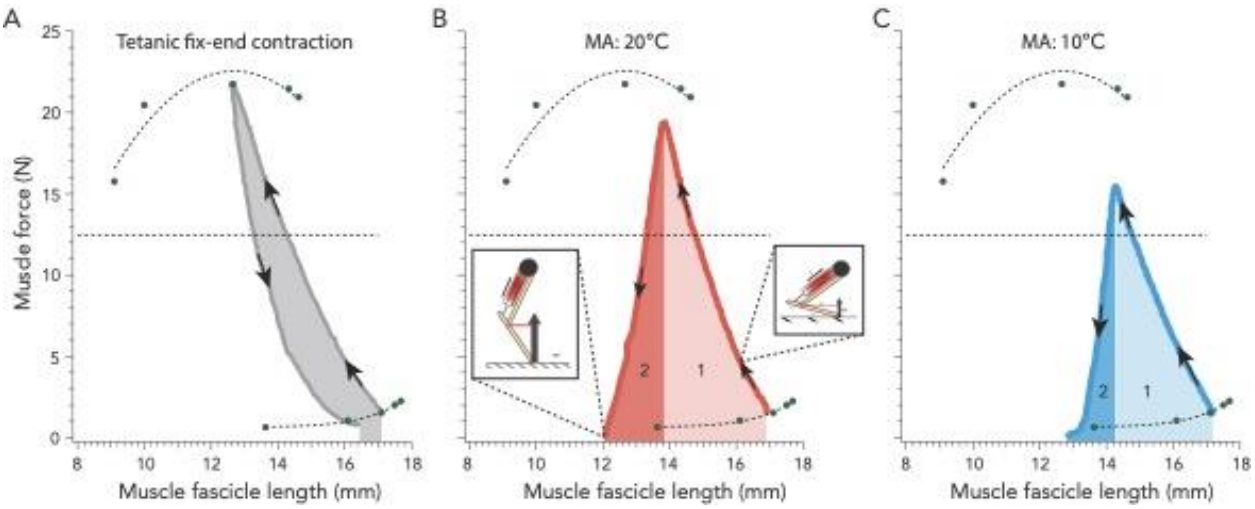

Figure 2.3: Representative workloops mapped into the force-length curve for a muscle. A) Workloop of a tetanic-fixed end contraction, B) workloop of an experimental contraction at 20°C, and C) workloop of an experimental contraction at 10°C. All three workloops began at a length of ~17mm with a passive force of ~2N and proceeded in the direction of the arrows. The opaque shaded area in B) and C) corresponds to the work done during the loading phase (indicated by 1). The horizontal dashed line indicates the unlatching threshold for this muscle. For unlatching to initiate the muscle needed to reach this force. The muscle overshoots this threshold, and the amount of overshoot varied with temperature. During this time, the inertia of the limb introduced a delay in unlatching and allowed additional work to be stored. The solid shaded area in B) and C) corresponds to the muscle fascicle work done during the unloading phase when the joint is extending (indicated by 2). When the muscle could not reach the unlatching force threshold the contraction would proceed as a normal tetanic fixed-end contraction.

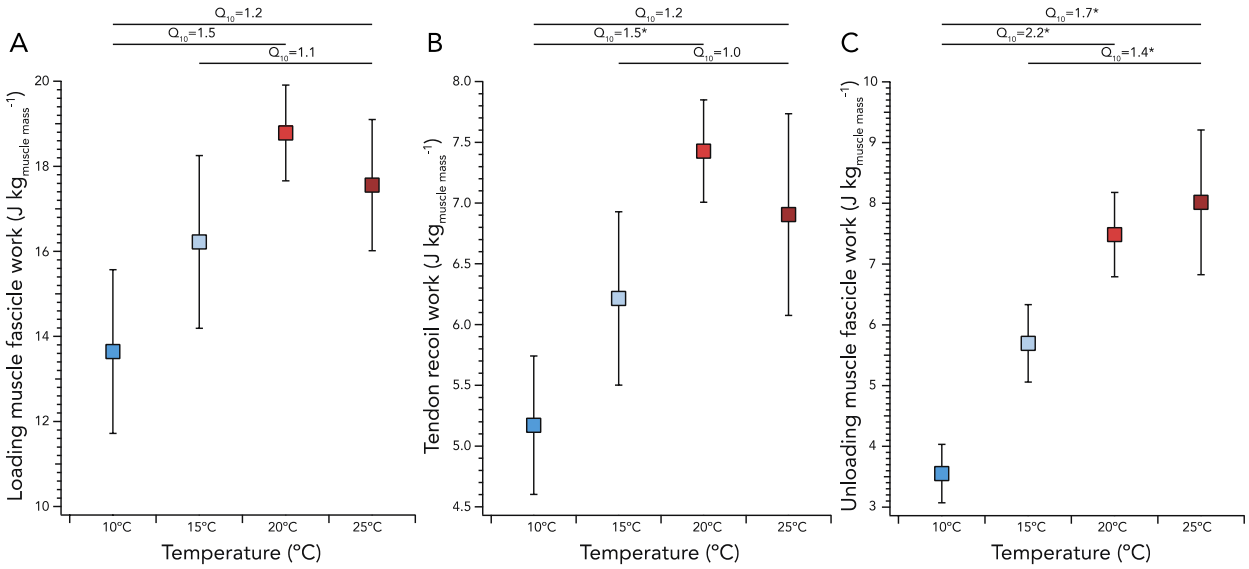

Figure 2.4: Mass-specific work as a function of temperature. A) Loading muscle fascicle work, B) tendon recoil work, C) unloading muscle fascicle work plotted against temperature. Boxes are means and the error bars are S.E.M. Temperature coefficients significantly different from 1.0 are indicated with an asterisk.

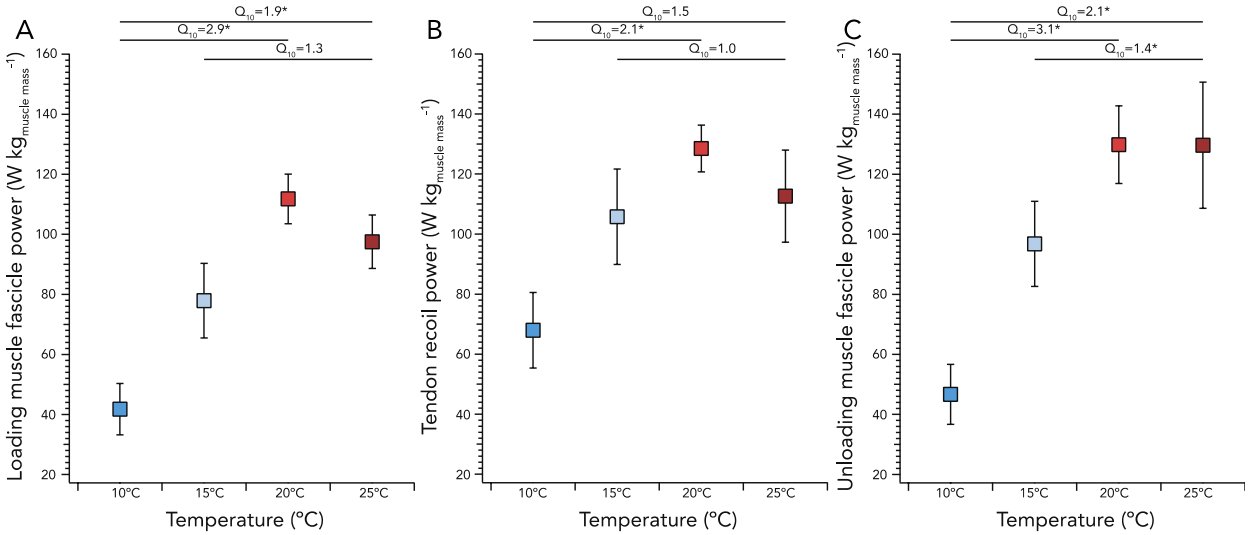

Figure 2.5: Mass-specific power as a function of temperature. A) Loading muscle fascicle power, B) tendon recoil power, and C) unloading muscle fascicle power plotted against temperature. Boxes are means and the error bars are S.E.M. Temperature coefficients significantly different from 1.0 are indicated with an asterisk.

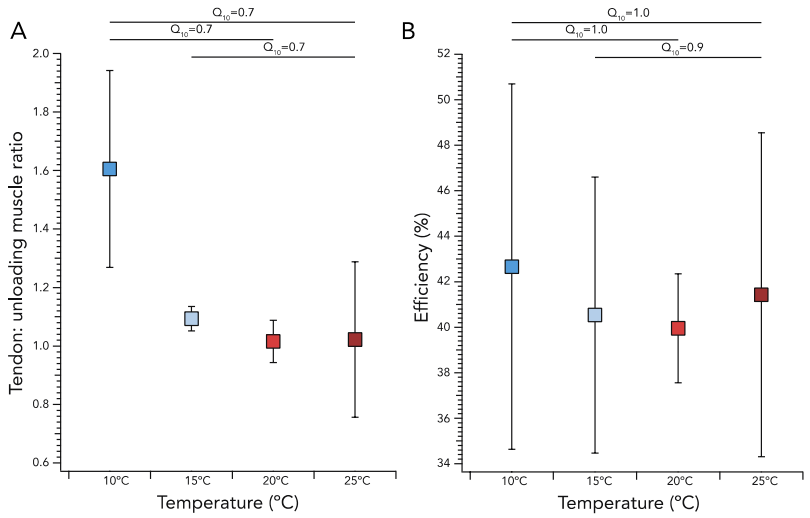

Figure 2.6: Temperature effects on tendon:unloading muscle fascicle work ratio and tendon efficiency. A) Tendon recoil work:unloading muscle fascicle work ratio and B) efficiency plotted against temperature. Boxes are means and the error bars are S.E.M. Temperature coefficients significantly different from 1.0 are indicated with an asterisk.

CHAPTER 3

Quantifying the relative contributions of muscular and elastic energy contributions during a frog jump

INTRODUCTION

Jumping is a powerful movement that requires a tremendous amount of mechanical energy (Marsh 1994; Marsh and John-Alder 1994; Peplowski and Marsh 1997; Aerts 1998; Roberts and Marsh 2003; Henry et al. 2005; Roberts and Azizi 2011; Roberts et al. 2011; Farley et al. 2019; Bertone et al. 2022). Previous studies have shown that jumping power often exceeded what was physiologically possible by typical skeletal muscles even when accounting for the mass of all the hind limb muscles (Marsh 1994; Marsh and John-Alder 1994; Aerts 1997; Peplowski and Marsh 1997; Roberts and Marsh 2003; Henry 2005; Roberts et al. 2011; Mendoza et al. 2020). Such studies indicated that the movements were powered by latch-mediation spring-actuation (LaMSA) mechanisms which redistributed muscle work over a shorter period of time.

To meet the energy requirements for a jump some organisms use LaMSA mechanisms where energy is temporarily stored in the elastic deformations of biological tissues and then quickly released to actuate motion (Ilton et al. 2018; Longo et al. 2019; Patek 2023). The LaMSA mechanism functions through the interaction of four key components: a latch, spring, motor, and projectile (Ilton et al. 2018; Longo et al. 2019; Patek 2023). For the mechanism to initiate the system must first become latched (i.e., latching phase). Then, the latch resists motion of a joint or body segment and allows the muscle to contract against surrounding elastic structures, storing energy in elastic deformations (i.e., loading phase). Latch removal initiates the recoil of elastic structures (i.e., spring actuation phase) and the release of stored energy to

accelerate the projectile to takeoff (i.e., ballistic phase) (Ilton et al. 2018; Longo et al. 2019; Patek 2023). While the general understanding of how this mechanism works is understood in simplified models (Ilton et al. 2018; Divi et al. 2020), it is still not well understood how interactions amongst the components leads to high-powered motion in biological organisms.

Studies examining biological LaMSA systems have characterized the motion into the phases of the mechanism and demonstrated the incredible reduction of time made possible by LaMSA (Patek 2023). For example, a study on larval beetles characterized the durations of the phases in the LaMSA mechanism and showed that the loading phase had an average duration of 0.22s, unlatching had an average duration of 5.5ms, and the energy release phase lasted on average 1.4 ms (Bertone et al. 2022). In locusts (*Schistocerca gregaria*) the loading phase lasted 800ms and unloading phase lasted 8ms (Burrows and Morris 2001). In snapping shrimp (*Alpheus heterochaelis*), the loading phase lasted 390ms and the unloading phase lasted 0.7ms (Longo et al. 2023). Smashing mantis shrimp loaded energy for about 300ms and unloaded in about 49μs (Patek et al. 2004; Patek and Caldwell 2005; Patek 2019). Together, these studies suggest that in these systems the work done by the energy loading muscles could only be done during the loading phase (i.e., to allow sufficient time to load elastic structures), and could not be supplemented by the loading muscles after unlatching because the duration of unloading would be too short for the muscle to contribute additional work.

In recent years, studies on the mechanics of LaMSA systems have improved our understanding of how the interactions between components leads to high powered movements. For example, a modeling study investigated how the LaMSA components interacted in a simplified jumper with a dynamic mechanical advantage latch and showed that the muscle could do more work in the presence of an elastic element (Olberding et al. 2019). Furthermore, they

showed that varying latch morphology and projectile mass had consequences for work and power outputs (Olberding et al. 2019). This work indicates that interactions between components have major consequences for the capacity to do work and power output (Olberding et al. 2019). Moreover, modeling studies showed that the type of latch and speed of unlatching determined whether energy would be amplified or attenuated demonstrating that the latch plays a critical role in mediating energy flow (Ilton et al. 2018; Abbott et al. 2019; Divi et al. 2020; Divi et al. 2023). While these studies have been informative in understanding the mechanics of LaMSA, no study to date has measured the flow of internal energy in a biological LaMSA system.

Frog are known to use LaMSA mechanisms to jump. Studies have shown that frogs jump with incredibly high instantaneous jumping power even when accounting for all the hind limb musculature (Marsh and John-Alder 1994; Peplowski and Marsh 1997; Roberts et al. 2011; Astley 2016; Mendoza et al. 2020). More strikingly, studies that compared normalized instantaneous jumping power indicated that jump power exceeded the power physiologically possible by skeletal muscle (Marsh 1994; Marsh and John-Alder 1994; Peplowski and Marsh 1997; Roberts et al. 2011; Astley 2016). Moreover, in vivo muscle studies in jumping frogs showed that the *plantaris longus* muscle (an ankle extensor and knee flexor) was active and shortened prior to any appreciable ankle joint motion suggesting that it was storing energy in elastic structures (Olson and Marsh 1998; Roberts and Marsh 2003; Azizi and Roberts 2010; Astley and Roberts 2012). To store energy, Astley and Roberts (2014) showed that frogs used a dynamic mechanical advantage latch where the mechanical advantage of extensor hind limb muscles was poor while the frog was in its resting posture (or energy loading posture) and improved as the hind limb joints extended. Additionally, in vivo muscle studies showed that the *plantaris longus* muscle continued to shorten during ankle joint extension suggesting that the

muscle was contributing work to the jump in addition to that being recoiled by elastic structures (Roberts and Marsh 2003; Azizi and Roberts 2010; Astley and Roberts 2012). While there is evidence suggesting that frogs use both LaMSA mechanisms and direct muscle contributions to jump, we still do not know how much energy is contributed by recoil of elastic structures nor do we know how much the muscle contributes during joint extension. Thus, in this study we measured the work contributed by the *plantaris longus* muscle throughout the jump and we quantified the relative contributions of elastic recoil and muscular work. Moreover, we examined relationships between jumping performance and work contributions across the phases of LaMSA to understand how various work contributions affected performance.

METHODS

Animals

Nine bullfrogs (mean±SEM; 238.546±6.519g) were purchased from a herpetological vendor (Rana Ranch, Idaho, USA). Frogs were group housed in 10-gallon aquariums and were fed crickets and mealworms *ad libitum* three times a week. Animal husbandry and use were approved by the University of California, Irvine Animal Care and Use Committee (protocol AUP-20-129).

Electronics

To measure force from the *plantaris longus* muscle, we constructed a leaf spring tendon buckle following the methods of Richards and Biewener (2007). Briefly we cut Dr. Pepper aluminum soda cans into (width x length) 3x7mm strips. We adhered two aluminum strips together with Scotch super glue. After the glue cured, we used sandpaper to smoothen sharp

edges. Next, we prepared the aluminum leaf spring surface with a Strain Gauge Prep Kit from Micro-Measurements (Wendell, NC, USA). After prepping the leaf spring surface, we used an adhesive from Micro-Measurements (M-bond 200 Adhesive Kit; Wendell, NC, USA) to adhere a 350 olms linear strain gauge (Micro-Measurements; Wendell, NC, USA) to the center of our leaf spring, and allowed it to cure for a minimum of 24 hours. After curing, we checked the strain gauge resistance with a multimeter to ensure that the strain gauge was within the functional range (349-351 olms). Once confirmed, we carefully soldered leads on the strain gauge, and we checked the resistance again. We connected the instrumented leaf spring to a Vishay amplifier (Raleigh, NC, USA) and checked that it balanced. Once confirmed, we applied an acrylic coating (GAUGEKOTE #8, Micro-Measurements; Wendell, NC, USA) over the strain gauge grid and allowed 4 hours to cure. Next, we applied 5-minute epoxy (DEVCON home; Solon, OH) to the solder joints to strengthen the connection and prevent lead breakage from the soldering joints. Once cured, we coated the entire leaf spring and solder joints with another acrylic coating to protect the strain gauge from fluids and other contaminants. We allowed this to cure for 24 hours.

The leads of sonomicrometry crystals (Sonometrics Corporation, London, ON, Canada) were cut to a length approximating the length from the animal's center of mass to the *plantaris longus* muscle's mid-belly. The tips of the leads were stripped by approximately 1mm to expose the wire and they were soldered into a 12-pin male circular micro-connector socket (Omnetics, Thief River Falls, MN). Leads from the leaf spring tendon buckle were also soldered into the 12-pin micro-connector. We tested the connector with associated hardware before sealing the soldering joints with 5-minute epoxy. Both ends of a small thread of Kevlar (~20mm) were

anchored to the curing epoxy to create a loop that was used to secure the micro-connector onto the animal's back with 6-0 silk.

Surgical procedures

Frogs were anaesthetized using a bath of buffered MS-222 (pH = ~7.8; tricain methanosulphonate, 1g L^{-1}). They were kept in the bath until the animal were unresponsive. To ensure that our frogs were properly anaesthetized we checked for righting responses and reflexes by placing the frogs on their backs and by pinching the hind limb toes (Duman and Azizi, 2023). Once anaesthetized, we made a small incision on the skin on the dorsal side approximately 2 cm proximal to the cloaca. We used this incision to subcutaneously thread the sonomicrometry crystals, leaf-spring tendon buckle transducers, and their leads into the right hind limb. A second incision was made on the skin covering the *medial gluteus magnus* muscle to help pass the electrodes from the lower trunk to the upper hind limb. A third incision was made on the skin covering the *plantaris longus* muscle near the muscle's origin. One sonomicrometry crystal was implanted near the muscle's origin along a fascicle and the second was implanted along the same fascicle more distally located (proximal to the aponeurosis, Fig. 3.1). Sonomicrometry transducers were secured with 6-0 silk. A fourth incision was made on the skin covering the muscle-tendon junction of the *plantaris longus*, which is a few centimeters proximal to the ankle joint. The leaf spring tendon buckle was carefully placed proximal to the muscle-tendon junctions and sutured to the aponeurosis sheet with 6-0 silk (Fig. 3.1). Once all electrodes were sutured in place a scarce amount of vet bond was applied to the suture knots for reinforcement. Incisions on the skin were closed with 3-0 silk and a scarce amount of vet bond was applied to the suture knots for reinforcement. Lastly, we used great caution to avoid damaging surrounding muscles and minimized damage to surrounding connective tissues and our target muscle.

Once the surgery was complete, frogs were gently rinsed with room temperature water and placed in a plastic critter's container with a thin film of water. Recovering frogs were in observation until they were able to move around freely in the container (~1 hour). Once fully recovered from anesthesia, the frogs were housed individually in a 10-gallon aquarium with access to clean water. On the day of surgery, the frogs were monitored every hour for 6-hours post-surgery, and then three times a day (e.g. morning, afternoon, and evening) the following days. We administered 0.3 cc mL^{-1} of 2 mg mL^{-1} of Carprofen for post-operative pain daily. We allowed the frogs a minimum of 24 hours post-surgery to recover before data collection. Frogs were only handled during data collection to reduce the possibility of sutures breaks or electrodes pulling out.

Jumping arena

We constructed a jumping arena of 2.4 m x 1.5 m (length x width). On one end, we place a platform of 0.15m x 0.15m x 0.006m (length x width x height) to have the frogs jump from a consistent location, and on the other end we place a cardboard box to give the frogs a refuge to jump towards. The platform was lined with sandpaper to improve grip and was bolted onto the arena to prevent platform motion artifact. One side of the arena was constructed with clear plexiglass to allow for video recording of the jump in lateral view. We used two Edgertronics high-speed video cameras to record the jump takeoff at 250 frames per second (Edgertronic). One camera recorded from the lateral view and the other from the frontal-lateral view. Our cameras were set to save recording of videos five seconds before trigger onset. We synchronized our cameras with a custom-made external trigger box. Our trigger box interfaced with our data acquisition board through a BNC cable, and this allowed us to synchronize video data with in vivo muscle measurements.

Jumping data collection

We carefully dried excess water from the frog's body and feet with a towel to reduce the possibility of slipping during a jump. To prevent crosstalk across channels, we carefully blew out the 12-pin micro-connector with an air canister to remove water from inside the connector. Next, we connected the micro-connector to the interfacing cable and placed the frog on the jump platform. We initiated data collection on Igor Pro (Wavemetrics, Lake Oswego, OR, USA) and allowed a few seconds to record baseline data before we began to encourage the frogs to jump. The sonomicrometry crystals measured fascicle length changes and the leaf spring tendon buckle measured muscle force. Frogs were jumped at least one day post-surgery and at most 4 days post-surgery. To collect as many jumps as possible, we jump the for approximately 2 hours every day (Astley et al. 2015). During data collection, the frogs were given at least 5 minutes to recover between each jump. After each day of jumping data collection, the frogs were hand-fed five crickets and returned to their enclosure to rest. Frogs were allowed 24 hours between data collection days to rest. All in vivo muscle data were collected in Igor Pro at a sampling rate of 10,000 Hz.

In-situ muscle preparation and leaf-spring buckle calibration

After jumping trials, the frogs were euthanized with a double-pithing protocol. Frogs we placed in a dissection tray, and we carefully removed skin from the limb with great care to not cut sensor leads. Once the limb was freed of skin, we isolated the sciatic nerve branch and threaded it through a custom-made nerve cuff for direct stimulation. Next, we detached the distal tendon of the *plantaris longus* muscle from the plantar fascia and placed a custom-made clamp approximately one millimeter below the muscle-tendon junction. We secured the frog in a rig suited for an in-situ muscle preparation. A three-pronged clamp was used to fix the femur

horizontally as to make a 90-degree angle with the *plantaris longus* muscle attached to a 50N servomotor (310C, Aurora Scientific, Cambridge, MA, USA). The muscle-tendon unit and the nerve were regularly soaked with anuran ringer's solution to prevent desiccation. We performed twitch contractions with increasing voltage (i.e., 1V increments) to find the voltage where force plateaued following methods from Mendoza and Azizi (2021). Once determined, we performed tetanic fixed-end contractions at variable starting lengths to characterize the force-length relationship of the muscle. We repeated this procedure with twitch contractions. To characterize the relationship between muscle force and leaf spring tendon buckle voltage we plotted force measured by the servomotor in newtons against force measured by the leaf spring tendon buckle in voltage. We fit a linear regression and used this equation to convert leaf spring tendon buckle force in voltage to newtons (Fig. 3.2). After in-situ measurements, the muscle was detached from the body and we measured muscle mass, pennation angle, and fascicle length.

Data processing

Jump videos were reviewed and selected for data processing based on specific criteria. Only videos where the frog did not slip and where both hindlimbs extended simultaneously were selected for processing. Jump videos were digitized on MATLAB with the DLTV5 digitizing toolbox (Hedrick 2008). We tracked points on the snout, knee, ankle, and toe. All videos were tracked starting three frames before any observable movements and three frames after toe-off. We used a custom MATLAB code to process digitized video files and calculate ankle joint angles for all jumps. Ankle joint angle files were exported from MATLAB as comma separated files and imported to Igor Pro. We calculated snout displacement with digitized files in Igor Pro and used the interpolate function to smoothen the data. Then, we differentiated these data to extract jump take-off velocity and acceleration, and multiplied velocity times acceleration to

calculate power. In Igor Pro, we used the camera trigger square wave to align kinematic data with in vivo muscle data.

In vivo muscle data processing

In vivo muscle data were trimmed starting at 200ms prior to the onset of muscle shortening to toe-off. Trimmed sonomicrometry and muscle force data were filtered with a low pass filter. Trimmed sonomicrometry data were converted to fascicle lengths in millimeter, and trimmed muscle force was converted from voltage to newtons.

We partitioned the in vivo muscle data into two phases: the loading phase and unloading phase. The loading phase started at active muscle shortening and ended at peak force. The unloading phase started at peak muscle force and ended at toe-off. We defined these phases according to the behavior of elastic structures. Because elastic structures are passive, and their length is dependent only on force, development of force during the loading phase until peak force would indicate that the elastic structures are lengthening (Mendoza and Azizi 2021). Moreover, in the unloading phase muscle force decreases indicating that the elastic structures are recoiling. Using this approach, we measured duration and muscle work during the loading and unloading phase.

We measured muscle fascicle work during the loading phase by calculating the area under the plot of loading muscle force against loading muscle fascicle length. We repeated this procedure for work during the unloading phase by calculating the area under the plot of unloading muscle force against unloading fascicle length. Work values were divided by muscle mass to calculate mass-specific work (Mendoza and Azizi 2021). We calculated total muscle work during the jump by adding loading muscle fascicle work and unloading muscle fascicle

work. Then, we used total muscle fascicle work to calculate relative loading and unloading work by dividing both quantities by total muscle fascicle work. To calculate the work returned by the elastic structures, or tendon recoil work, we used efficiency data from Olberding et al. (unpublished). Specifically, we assumed that the elastic structures returned 70% of the work stored as elastic energy.

Finally, we calculated loading muscle fascicle power by dividing loading muscle fascicle work by loading time. We calculated tendon recoil power by dividing tendon recoil work by unloading time. Lastly, we calculated unloading muscle fascicle power by dividing unloading muscle fascicle work by unloading time.

STATISTICS

All statistics were performed in R studio (http://www.R-project.org/). We used linear mixed models (package lme4; Bates et al., 2015) to assess whether there were differences in duration across the loading and unloading phase. In these models duration was the dependent variable and the loading and unloading phase were the independent variable. Individuals were treated as random effects. Additionally, we used linear mixed effect models to assess whether work and power differed across the type (i.e., loading muscle fascicle, tendon, and unloading muscle fascicle). In these models work and power were the dependent variables and type was the independent variable. Individuals were treated as random effects. Moreover, we used linear mixed effects models to examine the relationship between takeoff velocity and work and power during the loading and unloading phase. In these models takeoff velocity was the dependent variable and work and power during the loading and unloading phase were the independent variables. Individuals were treated as random effects. Each model was compared to a null model and AIC scores were used to select the model with the most explanatory power. In all but four

cases the alternate model had more explanatory power than the null model, and in the four cases we determined that there was no relationship between our independent and dependent variables.

RESULTS

An example time series of a jump is shown in figure 3.3A. Prior to any appreciable ankle extension, the muscle was shortening and developing force. During ankle extension, the muscle fascicles continued to shorten, and the muscle generated force (although decaying) until the frog became ballistic (Fig. 3.3A). Figure 3.3B shows an example workloop of the jump. The muscle fascicles started at a length of 25.8mm and began to shorten while force developed until peak force. The area under the curve was the work done by the muscle fascicles during the loading phase. From peak force until toe-off the muscle fascicles continued to shorten while muscle force decayed. The area under this curve was the work done by the muscle fascicles during unloading. Collectively, the workloop indicated that the *plantaris longus* muscle did positive work during the entirety of the jump (Fig. 3.3B).

Mean loading time was (mean ± S.E.M.) 0.123 ± 0.005 seconds and mean unloading time 0.047 ± 0.002 seconds (Fig. 3.4). Mean loading time significantly differed from mean unloading time (Fig. 3.4; lme, $p<0.05$). Mean loading muscle fascicle work was 9.321 ± 0.445 J $kg_{muscle\ mass}^{-1}$, unloading muscle fascicle work was 4.200 ± 0.385 J $kg_{muscle\ mass}^{-1}$, and mean tendon recoil work was 6.524 ± 0.312 J $kg_{muscle\ mass}^{-1}$ (Fig. 3.5). In relative terms, the muscle fascicles contributed on average 72.245 ± 1.722% of the work during the loading phase and 27.549 ± 1.722% of the work during the unloading phase. During the unloading phase the muscle fascicles contributed 33.951 ± 1.939% of the work and tendon recoil contributed 66.049 ± 1.939% of the work. Mean loading muscle fascicle work was significantly different from tendon recoil work

and unloading muscle fascicle work (Fig. 3.5; lme, $p<0.05$). Moreover, tendon recoil work was significantly different from unloading muscle fascicle work (Fig. 3.5; lme, $p<0.05$).

Mean loading muscle fascicle power was 90.431 ± 5.699 W $kg_{muscle\ mass}^{-1}$, mean unloading muscle fascicle power was 101.691 ± 9.560 W $kg_{muscle\ mass}^{-1}$, and mean tendon recoil power was 189.217 ± 14.972 W $kg_{muscle\ mass}^{-1}$ (Fig. 3.6). Tendon recoil power was significantly different from loading muscle fascicle power and unloading muscle fascicle power (Fig. 3.6; lme, $p<0.05$). Loading muscle fascicle power was not significantly different from unloading muscle fascicle power (Fig. 3.6; lme, $p>0.05$).

Takeoff velocity had a significant positive relationship with loading muscle work and there was significant individual variation (Fig. 3.7A; $R^2 = 0.58$, lme, $p<0.05$). Takeoff velocity showed a significant positive relationship with tendon recoil work and showed significant individual variation (Fig. 3.7B; $R^2 = 0.58$, lme, $p<0.05$). Takeoff velocity did not show a relationship with unloading muscle work (Fig. 3.7C). Takeoff velocity showed a significant positive relationship with total muscle fascicle work (Fig. 3.7D; $R^2 = 0.60$, lme, $p<0.05$). Moreover, loading muscle power had a significant positive relationship with takeoff velocity and there was significant individual variation (Fig. 3.8A; $R^2 = 0.69$, lme, $p<0.05$). Tendon recoil power did not show a relationship with takeoff velocity (Fig. 3.8B). Unloading muscle power did not show a relationship with takeoff velocity (Fig. 3.8C). Total muscle fascicle power showed a significant positive relationship with takeoff velocity (Fig. 3.8D; $R^2 = 0.69$, lme, $p<0.05$).

Finally, across all the jumps analyzed, we found that 62% of the time the *plantaris longus* muscle did 70-100% of the total muscle fascicle work during the loading phase, 28% of the time they did 50-69% of the total muscle fascicle work during the loading phase, and 10% of the time

they did 30-49% of the total muscle fascicle work during the loading phase. Average takeoff velocity across these ranges was 1.859±0.048, 1.962±0.080, and 1.740±0.067 m s^{-1}, respectively.

DISCUSSION

In this study we were interested in investigating how the LaMSA mechanism in frog jumping compared to more idealized LaMSA. We characterized our data using the LaMSA framework and discovered that the anuran jumping mechanism generally followed this framework with some key deviations that are likely present in other animals that jump by extending their limbs (Ilton et al. 2018; Longo et al. 2019; Patek 2023). Astley and Roberts (2014) demonstrated that frogs used a dynamic mechanical advantage latch to store elastic energy, where unlatching was dependent on the leverage of the extensor muscles involved in elastic energy storage. In their resting posture, the bullfrogs' hindlimb joints (i.e., the hip, knee, and ankle) were fully flexed and latched (Astley and Roberts 2014). While the frogs sat in their resting posture, the *plantaris longus* began shortening and generating force indicating that the muscle fascicles were doing work and that the mechanism was in the spring loading phase (Fig. 3.3A). In contrast to the idealized LaMSA mechanism, the frogs' mechanism did not include a latched phase (Ilton et al. 2018; Longo et al. 2019; Patek 2023). Instead, the start of the spring loading phase also initiated unlatching, which resulted in the immediate transition from spring loading into the actuation phase. This difference was a consequence of the unlatching mechanics of the latch, which required the energy loading muscles to reach a force threshold to unlatch and start motion. Therefore, once these muscles began developing force and storing energy in the elastic elements, they also began the process of unlatching (Roberts and Marsh 2003; Astley and Roberts 2014; Olberding et al. 2019). Additionally, because the spring loading phase was dependent on the time it took the muscles to develop sufficient force to unlatch, spring loading

was time-limited as previously thought by Rosario et al. (2016). Moreover, our work showed that the muscle continued to shorten and generate force during ankle joint extension (Fig. 3.3A and 3.3B). This additional work contribution from the muscle was also a consequence of the unlatching mechanics. Because the muscle was still shortening and generating force at unlatching, the muscle was able to contribute additional work until the frog left the ground. This is distinct from other biological LaMSA systems, which are thought to have time for the muscle to deactivate and become fully relaxed before unlatching and actuation (Burrows and Morris 2001; Patek et al. 2004; Patek and Caldwell 2005; Ilton et al. 2018; Patek 2019; Longo et al. 2019; Bertone et al. 2022; Longo et al. 2023; Patek 2023). Taken together, our work demonstrated that frog jumps are driven by both elastic recoil and direct muscle contributions as previously suggested by Roberts and Marsh (2003), Azizi and Roberts (2010), and Astley and Roberts (2012) and Sutton et al. (2019) (Fig. 3.3). Moreover, the jumping mechanism in frogs highlights how tightly coupled the LaMSA components are in this system, and how their complex interactions influence each other and leads to substantial variability.

A hallmark of LaMSA is the cascading reduction of time (Ilton et al. 2018; Longo et al. 2019; Patek 2023). Studies on LaMSA systems indicate that the energy storage period is often orders of magnitude longer than the period of energy release highlighting the incredible reduction of time achieved by delivering energy using spring recoil. For example, Bertone et al. (2022) showed that in larvae beetles the loading phase lasted on average 0.22s and unloading lasted on average 1.4ms. Moreover, in locusts (*Schistocerca gregaria*) the loading phase lasted up to 800ms and unloading phase lasted 8ms (Burrows and Morris 2001). In snapping shrimp (*Alpheus heterochaelis*), the loading phase lasted 390ms and the unloading phase lasted 0.7ms (Longo et al. 2023). Smashing mantis shrimp loaded energy for about 300ms and unloaded in

about 49μs (Patek et al. 2004; Patek and Caldwell 2005; Patek 2019). In this study we found that the loading phase lasted on average 123ms, and the unloading phase lasted on average 47ms (Fig. 3.4). The total duration was in good agreement with previous studies that have measured jumps in bullfrogs (Olson and Marsh 1998). Moreover, the asymmetry in durations was not as extreme as in the systems described above because frog jumps used both spring recoil and direct muscle contributions to actuate the jump. Therefore, for the muscle to contribute energy to the jump after unlatching the unloading phase would require relatively longer durations to accommodate the time needed by the muscle to do work and the muscle would have to operate with high power.

In this study we investigated the relative work contributions of muscle and tendon in the *plantaris longus* MTU during frog jumping. We found that the *plantaris longus* muscle fascicles contributed the most work during the loading phase. Specifically, on average they did approximately 9.3 J $kg_{muscle\ mass}^{-1}$ of work during the loading phase of the jump which amounted to approximately 72% of the total work done by the muscle during the entire jump. Moreover, during the unloading phase the muscle fascicles contributed on average approximately 4.2 J $kg_{muscle\ mass}^{-1}$ which was approximately 28% of the total work done by the muscle fascicles during the entire jump. When we interrogated the work done by the muscle fascicles and tendon recoil during the unloading phase, we found that tendon recoil contributed the most work. We found that tendon recoil contributed on average approximately 66% and the muscle fascicles contributed approximately 34% of the total work done during the unloading phase of the jump. Moo et al. (2017) was the first study to measure both *in vivo* muscle fascicle length changes and muscle force in the *plantaris longus* muscle during a frog jump. While they did not use their novel data to examine work, their time series data indicated that total muscle fascicle work for a

jump was approximately 13.3 J $kg_{muscle\ mass}^{-1}$, which is consistent with values measured in this study. Moreover, while it is not possible to compare these data to other biological LaMSA systems because no other study has characterized the internal energy of a behavior driven by LaMSA, *in vivo* measurements of muscle work during cyclical motion exist that could be used for comparison (e.g. Biewener and Corning 2001; Daley and Biewener 2003; Gabaldon et al. 2004; Richards and Biewener 2007; McGuigan et al. 2009; Eng et al. 2019). Most of these studies have measured muscle work as it related to changes in mechanical demand with grade (Biewener and Corning 2001; Daley and Biewener 2003; Gabaldon et al. 2004; McGuigan et al. 2009; Eng et al. 2019), and here we explicitly focused on data from animals moving on an incline. We focused exclusively on incline locomotion because the muscles involved in locomotion would have to generate mechanical energy to propel them forward and upward which is more like jumping than level or decline locomotion (Roberts and Azizi 2011). McGuigan et al. (2009) showed that when the African pygmy goats (*Capra hircus L.*) were trotting up an incline the *lateral gastrocnemius*, *medial gastrocnemius*, and *superficial digital flexor* did 8.25, 7.46, and 3.16 J $kg_{muscle\ mass}^{-1}$ of net work, respectively. Daley and Biewener (2003) showed that in guinea fowl when running on an incline the *lateral gastrocnemius* did 12.0 J $kg_{muscle\ mass}^{-1}$ of net work. Similarly, Gabaldon et al. (2004) showed that the *lateral gastrocnemius* in turkey did 7.0 J $kg_{muscle\ mass}^{-1}$ of net work during incline running. Eng et al. (2019) characterized the work done by the *medial gastrocnemius* and *plantaris* muscles during incline trotting in rats (*Rattus norvegicus*) and showed that they did 1.8 and 3.0 J $kg_{muscle\ mass}^{-1}$ of net work. Biewener and Corning (2001) showed that the *lateral gastrocnemius* of mallard ducks (*Anas platyrhynchos*) did on average 13.1 and 4.8 J $kg_{muscle\ mass}^{-1}$ of net work during walking and swimming, respectively. Lastly, Richards and Biewener (2007) showed that in African clawed

frogs (*Xenopus laevis*) the *plantaris longus* muscle did 0.88 – 21.50 J $kg_{muscle\ mass}^{-1}$ of net work while swimming. Thus, while the behaviors examined here are all cyclical and are not known to use LaMSA mechanisms the work done by these muscles is consistent with what we measured and provides confidence that our measurements of work were within reason. Moreover, this work highlights that LaMSA behaviors are not exceptionally high energy, but instead leverage the reduction of time afforded by using springs to deliver high powered movements (Ilton et al. 2018, Longo et al. 2019; Patek 2023).

Additionally, we examined the relationship between jump takeoff velocity (a performance metric) and work during the loading and unloading phase to understand how well these contributions explained jump performance. We found that jump takeoff velocity had a significant positive relationship with loading muscle work and tendon recoil work, and both relationships showed significant individual variation (Fig. 3.7A and 3.7B). Furthermore, when examining the relationship between takeoff velocity and unloading muscle fascicle work, we found that the null model had more explanatory power than unloading muscle fascicle work (Fig. 3.7C). While we find no relationship between unloading muscle fascicle work and jump takeoff velocity, our data showed that there was variation in the amount of unloading work contributed across jumps. This variation is due to the latch and the time available to do work during the loading phase. If the latch allowed time to sufficiently load the spring, then the frog would takeoff too quickly to allow for significant muscle work contributions during unloading. If the latch released early, then the muscle would have more time to contribute work during the unloading phase. Our data suggests that there is a balancing act between the work done by the muscle during the loading and unloading phase that is set by the latch and required to jump. Our work showed that 62% of the time the *plantaris longus* muscle did 70-100% of the muscle

fascicle work during the loading phase, and 38% of the time it did 30-69% of the muscle fascicle work during the loading phase. This indicates that in majority of the jumps examined here the *plantaris longus* muscle did most of the work during the loading phase. Moreover, this work shows that the unloading muscle fascicle work could supplement energy to the jump when not enough energy was stored during the loading phase (i.e., because it is time-limited; Rosario et al. 2016). Additionally, these data suggest that unloading muscle fascicle work could serve to provide control to the jump after unlatching, which may aid in changing jump direction or performance. Thus, here we propose that there is a balancing act between the work done during the loading and unloading phase, where the *plantaris longus* muscle will contribute most if not all the work during the loading phase when conditions are ideal or will contribute more during the unloading phase in less ideal conditions.

LIMITATIONS AND FUTURE DIRECTIONS

In this study we were unable to measure the recoil of elastic structures. Former studies on tendon have shown that when its loaded cyclically it can return up 90% of the energy stored, yet elastic structures in LaMSA systems do not undergo cyclical loading (Ker 1981; Alexander 1988). Therefore, we assumed an efficiency of 70% based on isolated tendon recoil experiments performed on bullfrog tendons (Olberding et al. unpublished data). To test the validity of this assumption future studies will need to load and unload elastic tissues (e.g. tendon and aponeurosis) with biologically relevant durations and strains, and measure the efficiency of recoil. Moreover, in this study we examined the relationship between takeoff velocity and muscle and tendon work to understand whether work contributions from the loading and unloading phase could explain jump performance. While we found some positive relationships, our data also showed variation. Jumping is a complex movement that requires coordination of

muscles spanning multiple joints and work contributions from multiple extensor muscles (Olson and Marsh 1998). Thus, the variation observed in our data was likely due to other extensor hind limb muscles contributing work to the jump that were not measured in this study. Future work examining the work contributions of those muscles may find stronger relationships between muscle work and jump performance. Lastly, in this study we measured the work contributions of the *plantaris longus* muscle during frog jumps and aimed to understand how energy flowed through the system. However, our study lacked detailed joint kinematics and kinetic measurements that are required to achieve a holistic view of the frog jump mechanism. Thus, future studies will need to combine in vivo muscle measurements with kinematic and kinetic measurements to tease apart how internal and external energy flows in the frog jumping system.

CONCLUSIONS

In summary, here we measured in vivo muscle work from the *plantaris longus* muscle during frog jumps. We found that the frog jump mechanism generally followed the idealized LaMSA framework with some key deviations that arose from the latch mechanics. We found that the muscle stored energy during the spring loading phase and continued to contribute work after unlatching. We showed that on average the muscle stored 70% of the total muscle fascicle work as elastic energy and contributed 30% of the total muscle fascicle work after unlatching. Thus, our work showed that frog jumps used both LaMSA mechanisms and direct muscle contributions to jump.

FIGURES

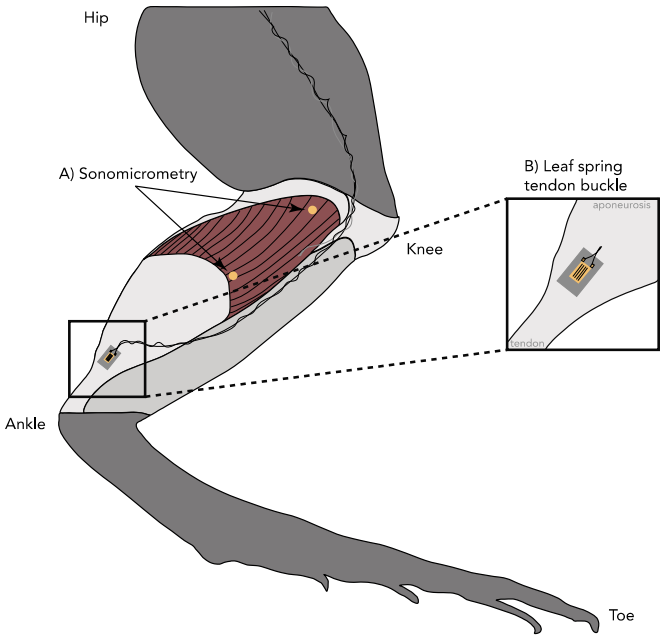

Figure 3.1: Illustration showing the right hind limb of a bullfrog and sensor placement on the *plantaris longus* muscle-tendon unit. A) Shows the approximate placing of the sonomicrometry crystals along a fascicle and B) shows the approximate placing of the leaf spring tendon buckle.

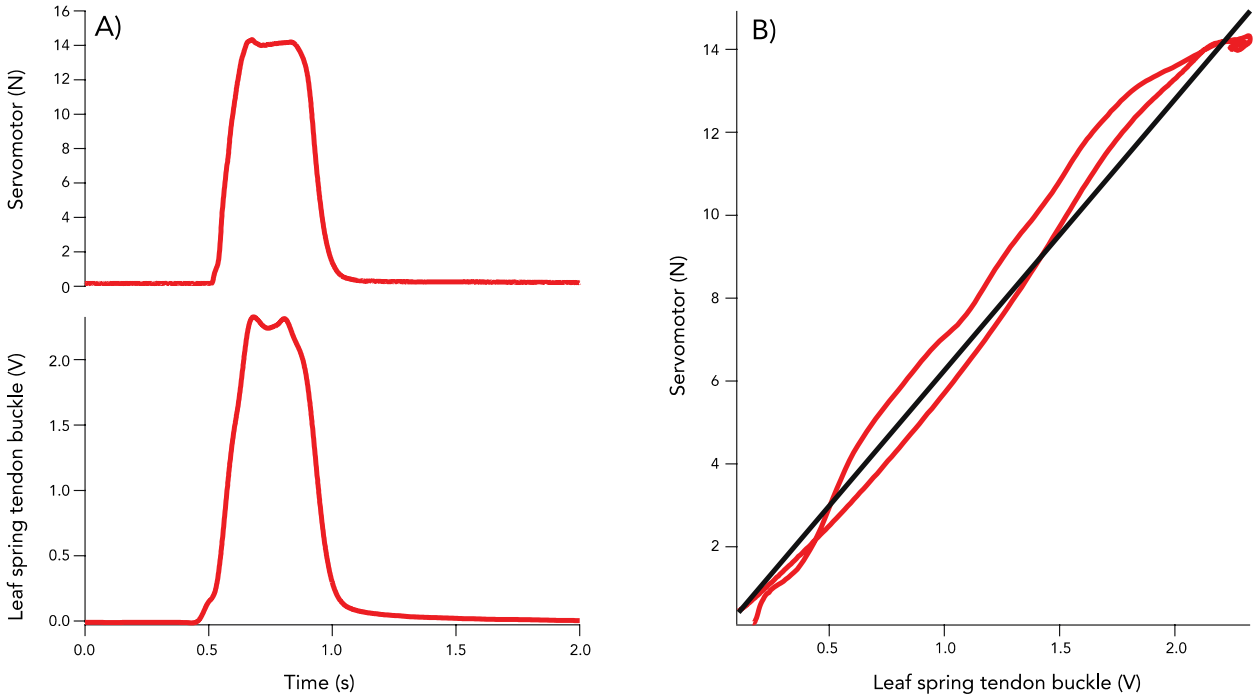

Figure 3.2: Example A) time series of servomotor force in newtons and leaf-spring tendon buckle force in voltage and B) calibration plot of servomotor force plotted against leaf-spring tendon buckle force. Buckle calibration yielded an R^2 value of 0.99.

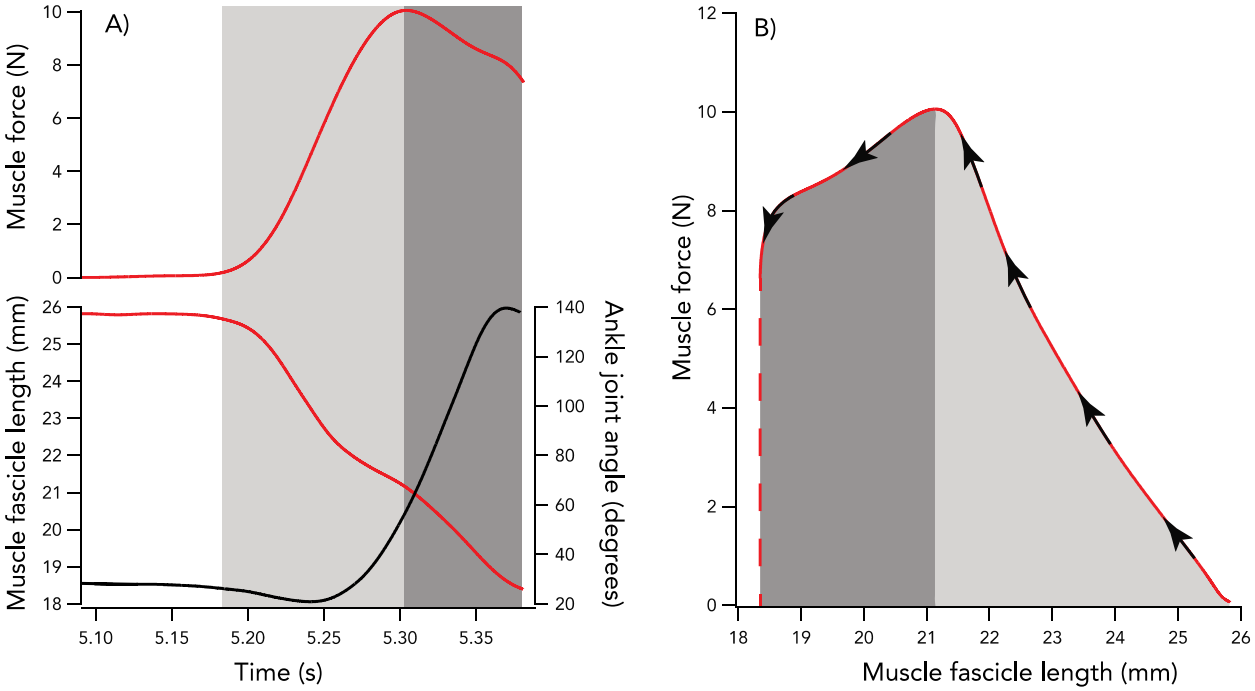

Figure 3.3: Time series and workloop for a frog jump. A) Time series demonstrating muscle force, fascicle length, and ankle joint angle during a frog jump. The light grey shading shows the loading phase and the dark grey shading show the unloading phase. The red traces correspond to muscle measurements and the black trace corresponds to kinematic measurements. B) Workloop showing the work done during the loading and unloading phase. The arrows indicate the direction of the workloop. The shading under the curves represents the work done during the loading (light grey) and unloading (dark grey) phase.

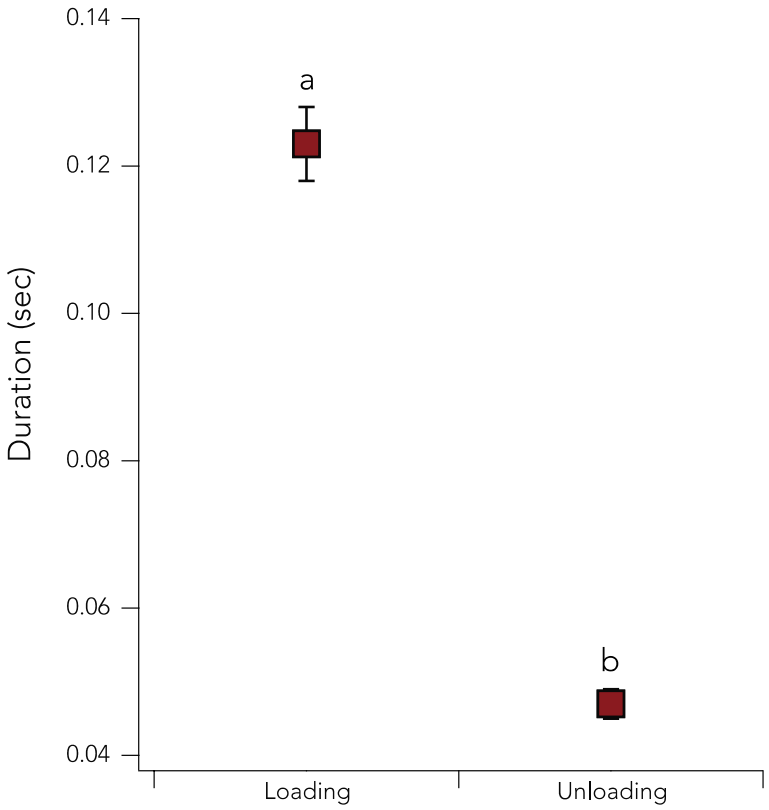

Figure 3.4: Boxplot showing loading and unloading phase durations for all the jumps analyzed. Duration was significantly different between the loading and unloading phase (as indicated by the lower-case letters; Lme, $p<0.05$).

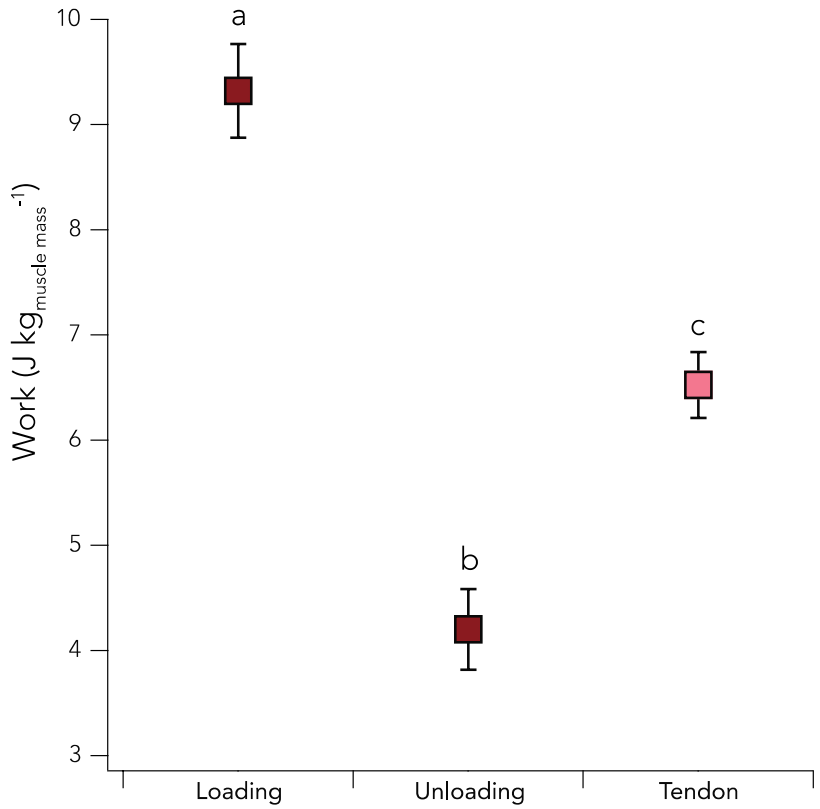

Figure 3.5: Boxplot showing loading, tendon, and unloading work for all the jumps analyzed. Work was significantly different across the three types (as indicated by the lower-case letters; Lme, $p<0.05$). Loading muscle fascicle work was significantly different from tendon recoil work and unloading muscle fascicle work (Lme, $p<0.05$). Tendon recoil work was significantly different from unloading muscle fascicle work (Lme, $p<0.05$).

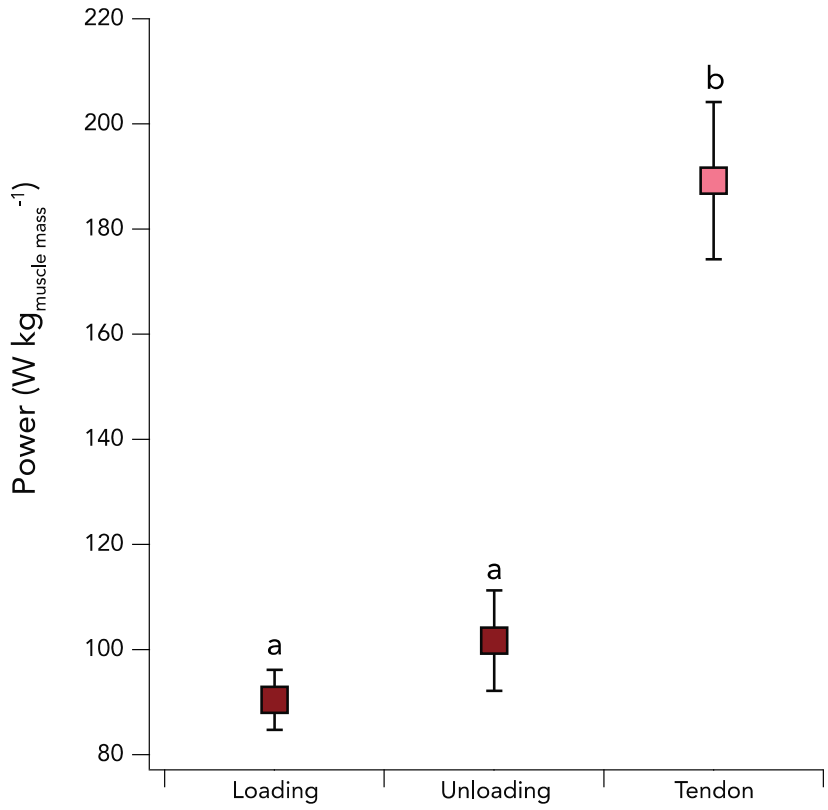

Figure 3.6: Boxplot showing loading, unloading, and tendon power for all the jumps analyzed. Tendon recoil power was significantly different from loading muscle fascicle power and unloading muscle fascicle power (as indicated by the lower-case letters; Lme, $p<0.05$). Loading muscle fascicle power was not significantly different from unloading muscle fascicle power (Lme, $p>0.05$).

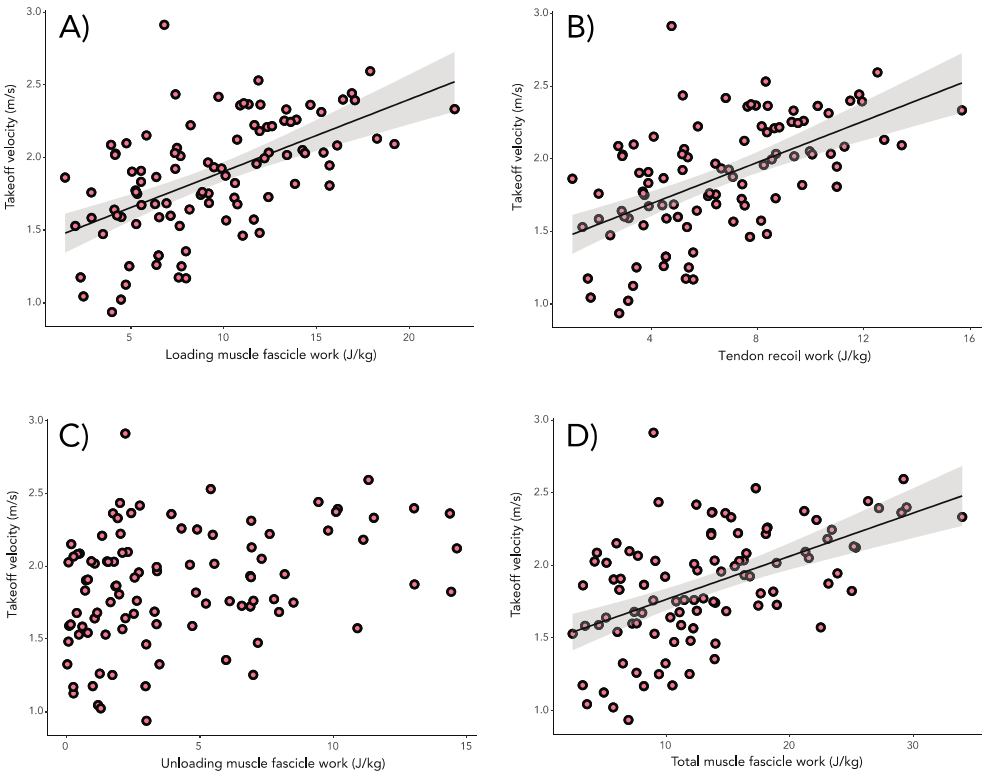

Figure 3.7: Scatterplots showing takeoff velocity as a function of A) loading muscle fascicle work, B) tendon recoil work, and C) unloading muscle fascicle work. A) Loading muscle fascicle work showed a significant positive relationship with takeoff velocity (R^2 = 0.58, lme, $p<0.05$). B) Tendon recoil work showed a significant positive relationship with takeoff velocity (R^2 = 0.58, lme, $p<0.05$). C) Unloading muscle fascicle work did not show a relationship with takeoff velocity (lme, $p>0.05$). D) Total muscle fascicle work showed a significant positive relationship with takeoff velocity (lme, $p<0.05$).

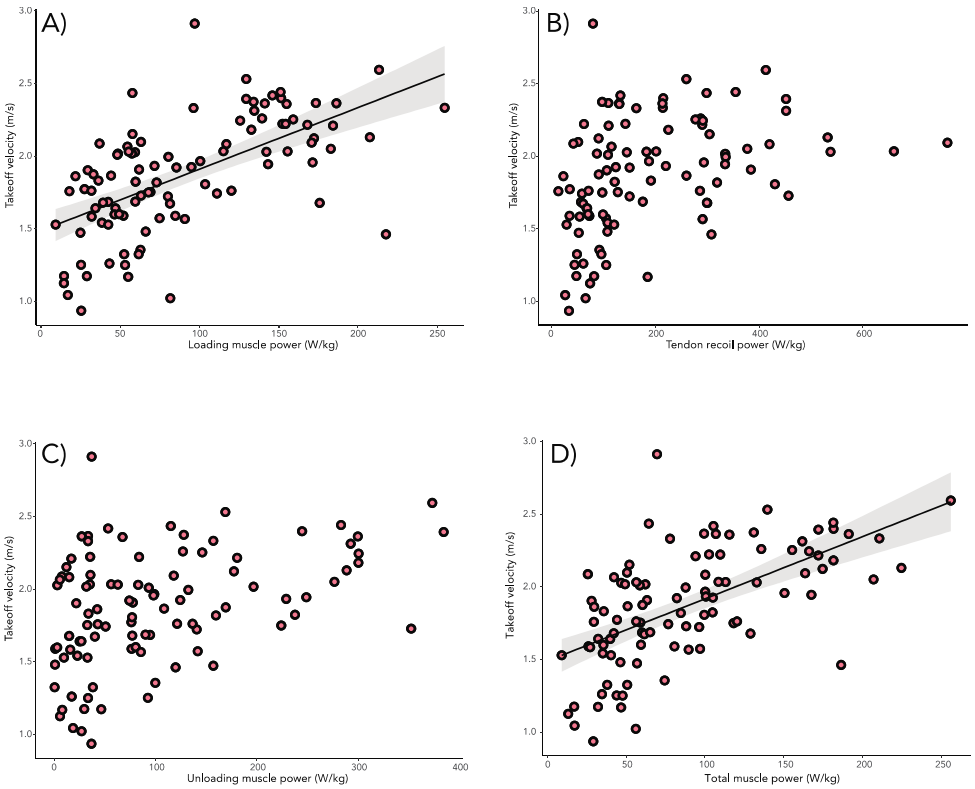

Figure 3.8: Scatterplots showing takeoff velocity as a function of A) loading muscle fascicle power, B) tendon recoil power, C) unloading muscle fascicle power, D) and total muscle fascicle power. A) Loading muscle fascicle power showed a significant positive relationship with takeoff velocity (R^2 = 0.69, lme, $p<0.05$). B) Tendon recoil power did not show a relationship with takeoff velocity (lme, $p>0.05$). C) Unloading muscle fascicle power did not show a significant relationship with takeoff velocity (lme, $p>0.05$). D) Total muscle fascicle power showed a significant relationship with takeoff velocity (R^2 = 0.69, lme, $p>0.05$).

REFERENCES

Abbott, E. M., Nezwek, T., Schmitt, D., and Sawicki, G. S. (2019). Hurry Up and Get Out of the Way! Exploring the Limits of Muscle-Based Latch Systems for Power Amplification. *Integrative and comparative biology*, 59, 1546–1558.

Acharya, R., Challita, E. J., Ilton, M., & Saad Bhamla, M. (2021). The ultrafast snap of a finger is mediated by skin friction. *Journal of the Royal Society Interface*, 18, 20210672.

Aerts, P. (1998). Vertical jumping in Galago senegalensis: the quest for an obligate mechanical power amplifier. *Philosophical Transactions of the Royal Society of London. Series B: Biological Sciences*, 353, 1607-1620.

Alexander, R. M. (1988). *Elastic mechanisms in animal movement* (Vol. 404). Cambridge: Cambridge University Press.

Anderson, C. V., and Deban, S. M. (2010). Ballistic tongue projection in chameleons maintains high performance at low temperature. *Proceedings of the National Academy of Sciences*, 107, 5495–5499.

Anderson, C. V., and Deban, S. M. (2012). Thermal effects on motor control and in vitro muscle dynamics of the ballistic tongue apparatus in chameleons. *Journal of Experimental Biology*, 215, 4345–4357.

Angilletta Jr, M. J., Niewiarowski, P. H., & Navas, C. A. (2002). The evolution of thermal physiology in ectotherms. *Journal of thermal Biology*, 27, 249–268.

Arellano, C. J., Konow, N., Gidmark, N. J., and Roberts, T. J. (2019). Evidence of a tunable

biological spring: elastic energy storage in aponeuroses varies with transverse strain in vivo. *Proceedings of the Royal Society B*, 286, 2018–2764.

Astley, H. C. (2016). The diversity and evolution of locomotor muscle properties in anurans. *Journal of Experimental Biology*, 219, 3163–3173.

Astley, H. C., and Roberts, T. J. (2012). Evidence for a vertebrate catapult: elastic energy storage in the plantaris tendon during frog jumping. *Biology letters*, 8, 386–389.

Astley, H. C., and Roberts, T. J. (2014). The mechanics of elastic loading and recoil in anuran jumping. *Journal of Experimental Biology*, 217, 4372–4378.

Astley, H. C. (2016). The diversity and evolution of locomotor muscle properties in anurans. *Journal of Experimental Biology*, 219, 3163–3173.

Astley, H. C., Abbott, E. M., Azizi, E., Marsh, R. L., and Roberts, T. J. (2013). Chasing maximal performance: a cautionary tale from the celebrated jumping frogs of Calaveras County. *Journal of Experimental Biology*, 216, 3947–3953.

Azizi, E., Brainerd, E. L., and Roberts, T. J. (2008). Variable gearing in pennate muscles. *Proceedings of the National Academy of Sciences*, 105, 1745–1750.

Azizi, E., and Roberts, T. J. (2010). Muscle performance during frog jumping: influence of elasticity on muscle operating lengths. *Proceedings of the Royal Society B: Biological Sciences*, 277, 1523–1530.

Azizi, E., and Roberts, T. J. (2014). Geared up to stretch: pennate muscle behavior during active lengthening. *Journal of Experimental Biology*, 217, 376–381.

Azizi, E., and Roberts, T. J. (2010). Muscle performance during frog jumping: influence of elasticity on muscle operating lengths. *Proceedings of the Royal Society B:*

Biological Sciences, 277, 1523–1530.

Bates, D., Machler, M., Bolker, B. M. and Walker, S. C. (2015). Fitting linear mixed-effects models using lme4. J. Stat. Software.67, 1.

Bennett, A. F. (1984). Thermal dependence of muscle function. *American Journal of Physiology-Regulatory, Integrative and Comparative Physiology*, 247, R217–R229.

Bennett, A. F. (1985). Temperature and muscle. *Journal of Experimental Biology*, 115, 333–344.

Bennett, A. F. (1990). Thermal dependence of locomotor capacity. *American Journal of Physiology-Regulatory, Integrative and Comparative Physiology*, 259, R253–R258.

Benjamini, Y., and Hochberg, Y. (1995). Controlling the false discovery rate: a practical and powerful approach to multiple testing. *Journal of the Royal statistical society: series B (Methodological)*, 57, 289–300.

Bertone, M.A., Gibson, J. C., Seago, A. E. ,Yoshida, T., Smith, A. A. (2022) A novel power-amplified jumping behavior in larval beetles (Coleoptera: Laemophloeidae). PLoS ONE 17:e0256509.

Biewener, A. A. (1998). Muscle function in vivo: a comparison of muscles used for elastic energy savings versus muscles used to generate mechanical power1. *American Zoologist*, 38, 703–717.

Biewener, A. A., and Corning, W. R. (2001). Dynamics of mallard (*Anas platyrynchos*) gastrocnemius function during swimming versus terrestrial locomotion. *Journal of*

Experimental Biology, 204, 1745-1756.

Biewener, A. A., and Roberts, T. J. (2000). Muscle and tendon contributions to force, work, and elastic energy savings: a comparative perspective. *Exercise Sport Sciences Reviews*, 28, 99–107.

Biewener, A., and Patek, S. (2018). *Animal locomotion*. Oxford University Press.

Blanco, M. M., and Patek, S. N. (2014). Muscle trade-offs in a power-amplified prey capture system. *Evolution*, 68, 1399–1414.

Booher, D. B., Gibson, J. C., Liu, C., Longino, J. T., Fisher, B. L., Janda, M., and Economo, E. P. (2021). Functional innovation promotes diversification of form in the evolution of an ultrafast trap-jaw mechanism in ants. *PLoS Biology*, 19, e3001031.

Burkholder, T. J., and Lieber, R. L. (2001). Sarcomere length operating range of vertebrate muscles during movement. *Journal of Experimental Biology*, 204, 1529–1536.

Burrows, M., and Morris, G. (2001). The kinematics and neural control of high-speed kicking movements in the locust. *Journal of Experimental Biology*, 204, 3471-3481.

Daley, M. A., and Biewener, A. A. (2003). Muscle force-length dynamics during level versus incline locomotion: a comparison of in vivo performance of two guinea fowl ankle extensors. *Journal of Experimental Biology*, *206*(17), 2941-2958.

Deban, S. M., and Richardson, J. C. (2011). Cold-blooded snipers: thermal independence of ballistic tongue projection in the salamander *Hydromantes platycephalus*. *Journal of Experimental Zoology Part A: Ecological Genetics and Physiology*, 315, 618–630.

Deban, S. M., and Lappin, A. K. (2011). Thermal effects on the dynamics and motor

control of ballistic prey capture in toads: maintaining high performance at low temperature. *Journal of experimental biology*, 214, 1333–1346.

Deban, S. M., Scales, J. A., Bloom, S. V., Easterling, C. M., O'Donnell, M. K., and Olberding, J. P. (2020). Evolution of a high-performance and functionally robust musculoskeletal system in salamanders. *Proceedings of the National Academy of Sciences*, 117, 10445–10454.

Deban, S. M., and Anderson, C. V. (2021). Temperature effects on the jumping performance of house crickets. *Journal of Experimental Zoology Part A: Ecological and Integrative Physiology*, *335*(8), 659-667.

Dick, T. J., and Clemente, C. J. (2016). How to build your dragon: scaling of muscle architecture from the world's smallest to the world's largest monitor lizard. *Frontiers in Zoology*, 13, 1–17.

Divi, S., Ma, X., Ilton, M., St. Pierre, R., Eslami, B., Patek, S. N., and Bergbreiter, S. (2020). Latch-based control of energy output in spring actuated systems. *Journal of the Royal Society Interface*, 17, 20200070.

Divi, S., Reynaga, C., Azizi, E., and Bergbreiter, S. (2023). Adapting small jumping robots to compliant environments. *Journal of the Royal Society Interface*, 20, 20220778.

Duman, A., and Azizi, E. (2023). Hindlimb muscle spindles inform preparatory forelimb coordination prior to landing in toads. Journal of Experimental Biology, 226, jeb244629.

Else, P. L., & Bennett, A. F. (1987). The thermal dependence of locomotor performance and muscle contractile function in the salamander *Ambystoma tigrinum nebulosum*. *Journal of Experimental Biology*, 128, 219–233.

Eng, C. M., Konow, N., Tijs, C., Holt, N. C., and Biewener, A. A. (2019). In vivo force–length and activation dynamics of two distal rat hindlimb muscles in relation to gait and grade. *Journal of Experimental Biology*, 222, jeb205559.

Farley, G. M., Wise, M. J., Harrison, J. S., Sutton, G. P., Kuo, C., and Patek, S. N. (2019). Adhesive latching and legless leaping in small, worm-like insect larvae. *Journal of Experimental Biology*, 222, jeb201129.

Gabaldón, A. M., Nelson, F. E., and Roberts, T. J. (2004). Mechanical function of two ankle extensors in wild turkeys: shifts from energy production to energy absorption during incline versus decline running. *Journal of Experimental Biology*, 207, 2277-2288.

Gordon, A. M., Huxley, A. F., and Julian, F. J. (1966). The variation in isometric tension with sarcomere length in vertebrate muscle fibres. *The Journal of physiology*, 184, 170–192.

Hedrick, T. L. (2008). Software techniques for two-and three-dimensional kinematic measurements of biological and biomimetic systems. *Bioinspiration & biomimetics*, 3, 034001.

Henry, H. T., Ellerby, D. J., and Marsh, R. L. (2005). Performance of guinea fowl *Numida meleagris* during jumping requires storage and release of elastic energy. *Journal of*

Experimental Biology, 208, 3293-3302.

Herzog, W. (2019). The problem with skeletal muscle series elasticity. *BMC Biomedical Engineering*, 1, 1–14.

Herrel, A., James, R. S., and Van Damme, R. (2007). Fight versus flight: physiological basis for temperature-dependent behavioral shifts in lizards. *Journal of Experimental Biology*, 210, 1762–1767.

Hertz, P. E., Huey, R. B., and Nevo, E. (1982). Fight versus flight: body temperature influences defensive responses of lizards. *Animal Behaviour*, 30, 676–679.

Hill, A. V. (1938). The heat of shortening and the dynamic constants of muscle. *Proceedings of the Royal Society of London. Series B-Biological Sciences*, 126, 136–195.

Hirano, M., and Rome, L. C. (1984). Jumping performance of frogs (*Rana pipiens*) as a function of muscle temperature. *Journal of Experimental Biology*, 108, 429–439.

Hyun N.P., Olberding J.P., De A., Divi S., Liang X., Thomas E. St. Pierre R., Steinhardt E., Jorge J., Longo S.J., Cox S.M., Mendoza E., Sutton G.P., Azizi E., Crosby A.J., Bergbreiter S., Wood R.J., Patek S.N. (2023). Spring and latch dynamics can act as control pathways in ultrafast systems. *Biomimetics and Bioinspiration,* 18(2) 026002.

Ilton, M., Bhamla, M. S., Ma, X., Cox, S. M., Fitchett, L. L., Kim, Y., Koh, J.S., Krishnamurthy, D., Kuo, C. Y., Temel, F.Z., Crosby, A.J., Prakash, M., Sutton, G.P., Wood, R.J., Azizi,

E., Bergbreiter, S., and Patek, S.N. (2018). The principles of cascading power limits in small, fast biological and engineered systems. *Science*, 360, eaao1082.

James, R. S. (2013). A review of the thermal sensitivity of the mechanics of vertebrate skeletal muscle. *Journal of Comparative Physiology B*, 183, 723–733.

John-Alder, H. B., Morin, P. J., and Lawler, S. (1988). Thermal physiology, phenology, and distribution of tree frogs. *The American Naturalist*, 132, 506–520.

Johnson, T. P., Bennett, A. F., and McLister, J. D. (1996). Thermal dependence and acclimation of fast start locomotion and its physiological basis in rainbow trout (*Oncorhynchus mykiss*). *Physiological Zoology*, 69, 276–292.

Ker, R. F. (1981). Dynamic tensile properties of the plantaris tendon of sheep (Ovis aries). *J Exp. Biol.* 93, 283–302.

Larabee, F. J., Gronenberg, W., and Suarez, A. V. (2017). Performance, morphology and control of power-amplified mandibles in the trap-jaw ant Myrmoteras (Hymenoptera: Formicidae). *Journal of Experimental Biology*, 220, 3062–3071.

Lin, D. C., McGowan, C. P., Blum, K. P., and Ting, L. H. (2019). Yank: the time derivative of force is an important biomechanical variable in sensorimotor systems. *Journal of Experimental Biology*, 222, jeb180414.

Longo, S. J., Cox, S. M., Azizi, E., Ilton, M., Olberding, J. P., St Pierre, R., and Patek, S. N. (2019). Beyond power amplification: latch-mediated spring actuation is an emerging framework for the study of diverse elastic systems. *Journal of Experimental Biology*,

222, jeb197889.

Longo, S. J., Ray, W., Farley, G. M., Harrison, J., Jorge, J., Kaji, T., Palmer, A. R., and Patek, S. N. (2021). Snaps of a tiny amphipod push the boundary of ultrafast, repeatable movement. *Current Biology*, 31, R116–R117.

Longo, S. J., St. Pierre, R., Bergbreiter, S., Cox, S., Schelling, B., and Patek, S. N. (2023). Geometric latches enable tuning of ultrafast, spring-propelled movements. *Journal of Experimental Biology*, 226, jeb244363.

Lutz, G. J., and Rome, L. C. (1996). Muscle function during jumping in frogs. I. Sarcomere length change, EMG pattern, and jumping performance. *American Journal of Physiology-Cell Physiology*, 271, C563–C570.

Marsh, R. L. (1994). Jumping ability of anuran amphibians. *Advances in veterinary science and comparative medicine*, *38*, 51–111.

Marsh, R. L., and John-Alder, H. B. (1994). Jumping performance of hylid frogs measured with high-speed cine film. *Journal of Experimental Biology*, 188, 131-141.

McGuigan, M. P., Yoo, E., Lee, D. V., and Biewener, A. A. (2009). Dynamics of goat distal hind limb muscle–tendon function in response to locomotor grade. *Journal of Experimental Biology*, 212, 2092-2104.

Mendoza, E., Azizi, E., and Moen, D. S. (2020). What explains vast differences in jumping power within a clade? Diversity, ecology and evolution of anuran jumping

power. *Functional Ecology*, 34, 1053–1063.

Mendoza, E., and Azizi, E. (2021). Tuned muscle and spring properties increase elastic energy storage. *Journal of Experimental Biology*, 224, jeb243180.

Mendez, J., and A. Keys (1960). Density and composition of mammalian muscle. Metabolism 9:184–188.

Moo, E. K., Peterson, D. R., Leonard, T. R., Kaya, M., and Herzog, W. (2017). In vivo muscle force and muscle power during near-maximal frog jumps. *PLoS One*, 12, e0173415.

Navas, C. A. (1996). Metabolic physiology, locomotor performance, and thermal niche breadth in neotropical anurans. *Physiological Zoology*, 69, 1481–1501.

Navas, C. A., James, R. S., Wakeling, J. M., Kemp, K. M., and Johnston, I. A. (1999). An integrative study of the temperature dependence of whole animal and muscle performance during jumping and swimming in the frog *Rana temporaria*. *Journal of Comparative Physiology B*, 169, 588–596.

Olberding, J. P., and Deban, S. M. (2017). Effects of temperature and force requirements on muscle work and power output. *Journal of Experimental Biology*, 220, 2017–2025.

Olberding, J. P., and Deban, S. M. (2018). Scaling of work and power in a locomotor muscle of a frog. *Journal of Comparative Physiology B*, 188, 623–634.

Olberding, J. P., Deban, S. M., Rosario, M. V., and Azizi, E. (2019). Modeling the determinants

of mechanical advantage during jumping: consequences for spring-and muscle-driven movement. *Integrative and Comparative Biology,* 59, 1515–1524.

Olberding J. P., and Deban, S. M. (2021). Thermal robustness of biomechanical processes. *Journal of Experimental Biology,* 224, 1–10.

Olson, J. M., and Marsh, R. L. (1998). Activation patterns and length changes in hindlimb muscles of the bullfrog *Rana catesbeiana* during jumping. *Journal of Experimental Biology*, 201, 2763–2777.

Otten, E. (1988). Concepts and models of functional architecture in skeletal muscle. *Exercise Sport Sciences Reviews*, 16, 89–138.

Patek, S. N., Korff, W. L., and Caldwell, R. L. (2004). Deadly strike mechanism of a mantis shrimp. *Nature*, 428, 819–820.

Patek, S. N., and Caldwell, R. L. (2005). Extreme impact and cavitation forces of a biological hammer: strike forces of the peacock mantis shrimp *Odontodactylus scyllarus*. *Journal of Experimental Biology*, 208, 3655–3664.

Patek, S. N., Dudek, D. M., and Rosario, M. V. (2011). From bouncy legs to poisoned arrows: elastic movements in invertebrates. *Journal of Experimental Biology*, 214, 1973–1980.

Patek, S. N. (2019). The power of mantis shrimp strikes: interdisciplinary impacts of an extreme cascade of energy release. *Integrative and Comparative Biology*, 59, 1573-1585.

Patek, S. N. (2023). Latch-mediated spring actuation (LaMSA): the power of integrated biomechanical systems. *Journal of Experimental Biology*, *226*(Suppl_1), jeb245262.

Peplowski, M. M., and Marsh, R. L. (1997). Work and power output in the hindlimb muscles of Cuban tree frogs *Osteopilus septentrionalis* during jumping. *The Journal of experimental biology*, 200, 2861–2870.

Putnam, R. W., and Bennett, A. F. (1982). Thermal dependence of isometric contractile properties of lizard muscle. *Journal of Comparative Physiology B*, 147, 11–20.

Rall, J. A., and Woledge, R. C. (1990). Influence of temperature on mechanics and energetics of muscle contraction. *American Journal of Physiology-Regulatory, Integrative and Comparative Physiology*, 259, R197–R203.

Reynaga, C. M., Eaton, C. E., Strong, G. A., and Azizi, E. (2019). Compliant substrates disrupt elastic energy storage in jumping tree frogs. *Integrative and Comparative Biology*, *59*(6), 1535–1545.

Richards, C. T., and Biewener, A. A. (2007). Modulation of in vivo muscle power output during swimming in the African clawed frog (*Xenopus laevis*). *Journal of Experimental Biology*, 210, 3147–3159.

Roberts, T. J., and Azizi, E. (2011). Flexible mechanisms: the diverse roles of biological springs in vertebrate movement. *Journal of Experimental Biology*, 214, 353-361.

Roberts, T. J., Abbott, E. M., and Azizi, E. (2011). The weak link: do muscle properties determine locomotor performance in frogs?. *Philosophical Transactions of the Royal Society B: Biological Sciences*, 366, 1488–1495.

Roberts, T. J., & Marsh, R. L. (2003). Probing the limits to muscle-powered accelerations: lessons from jumping bullfrogs. *Journal of Experimental Biology*, 206, 2567–2580.

Roberts, Thomas J. (2019). Some challenges of playing with power: does complex energy flow constrain neuromuscular performance? Integrative and comparative biology, 59, 1619–1628.

Rome, L. C. (1990). Influence of temperature on muscle recruitment and muscle function in vivo. *American Journal of Physiology-Regulatory, Integrative and Comparative Physiology*, 259, R210–R222.

Rosario, M. V., Sutton, G. P., Patek, S. N., and Sawicki, G. S. (2016). Muscle–spring dynamics in time-limited, elastic movements. *Proceedings of the Royal Society B: Biological Sciences*, 283, 2016–1561.

Rosin, S., and Nyakatura, J. A. (2017). Hind limb extensor muscle architecture reflects locomotor specialisations of a jumping and a striding quadrupedal caviomorph rodent. *Zoomorphology*, 136, 267–277.

Sacks, R. D., and Roy, R. R. (1982). Architecture of the hind limb muscles of cats: functional significance. *Journal of Morphology*, 173, 185–195.

Sandusky, P. E., and Deban, S. M. (2012). Temperature effects on the biomechanics of prey capture in the frog *Rana pipiens*. *Journal of Experimental Zoology Part A: Ecological Genetics and Physiology*, 317, 595–607.

Scales, J. A., O'Donnell, M. K., and Deban, S. M. (2017). Thermal sensitivity of motor

control of muscle-powered versus elastically powered tongue projection in salamanders. *Journal of Experimental Biology*, 220, 938–951.

Sutton, G. P., Mendoza, E., Azizi, E., Longo, S. J., Olberding, J. P., Ilton, M., and Patek, S. N. (2019). Why do large animals never actuate their jumps with latch-mediated springs? Because they can jump higher without them. *Integrative and comparative biology*, 59, 1609–1618.

Swoap, S. J., Johnson, T. P., Josephson, R. K., and Bennett, A. F. (1993). Temperature, muscle power output and limitations on burst locomotor performance of the lizard *Dipsosaurus dorsalis*. *Journal of Experimental Biology*, 174, 185–197.

Wainwright, P. C. and Bennett, A. F. (1992). The mechanism of tongue projection in chameleons: I. Electromyographic tests of functional hypotheses. *Journal of Experimental Biology*, 168, 1–21.

Whitehead, P. J., Puckridge, J. T., Leigh, C. M., and Seymour, R. S. (1989). Effect of temperature on jump performance of the frog *Limnodynastes tasmaniensis*. *Physiological Zoology*, 62, 937–949.

Zelik, K. E., and Franz, J. R. (2017). It's positive to be negative: Achilles tendon work loops during human locomotion. *Plos one*, 12, e0179976.